การเกิด N_2O และ SO_3 บนตัวเร่งปฏิกิริยา V-W-Mo/TiO_2 เตรียมโดยวิธีการเติมโลหะเป็นลำดับในระหว่างการรีดักชันแบบเลือกเกิดของ NO ด้วย NH_3

นางสาวกมลทิพย์ แซ่บ้าง

วิทยานิพนธ์นี้เป็นส่วนหนึ่งของการศึกษาตามหลักสูตรปริญญาวิศวกรรมศาสตรมหาบัณฑิต

สาขาวิชาวิศวกรรมเคมี ภาควิชาวิศวกรรมเคมี

คณะวิศวกรรมศาสตร์ จุฬาลงกรณ์มหาวิทยาลัย

ปีการศึกษา 2555

Formation of N_2O and SO_3 on V-W-Mo/TiO_2 Catalysts Prepared from Sequential Loading Method during the Selective Reduction of NO with NH_3

Miss Kamoltip Saebang

A Thesis Submitted in Partial Fulfillment of the Requirements
for the Degree of Master of Engineering Program in Chemical Engineering
Department of Chemical Engineering
Faculty of Engineering
Chulalongkorn University
Academic Year 2012

Thesis Title	FORMATION OF N_2O AND SO_3 ON V-W-MO/TIO_2 CATALYSTS PREPARED FROM SEQUENTIAL LOADING METHOD DURING THE SELECTIVE REDUCTION OF NO WITH NH_3
By	Miss Kamoltip Saebang
Field of Study	Chemical Engineering
Thesis Advisor	Associate Professor Tharathon Mongkhonsi, Ph.D.

Accepted by the Faculty of Engineering, Chulalongkorn University in Partial Fulfillment of the Requirements for the Master's Degree

…………………………….....Dean of the Faculty of Engineering
(Associate Professor Boonsom Lerdhirunwong, Dr.Ing.)

THESIS COMMITTEE

…………………………………Chairman
(Assistant Professor Suphot Phatanasri, Ph.D.)

…………………………………Thesis Advisor
(Associate Professor Tharathon Mongkhonsi, Ph.D.)

…………………………………Examiner
(Assistant Professor Anongnat Somwangthanaroj, Ph.D.)

…………………………………External Examiner
(Thongchai Glinrun, D.Eng.)

กมลทิพย์ แซ่บ้าง: การเกิด N_2O และ SO_3 บนตัวเร่งปฏิกิริยา V-W-Mo/TiO_2 เตรียมโดยวิธีการเติมโลหะเป็นลำดับในระหว่างการรีดักชันแบบเลือกเกิดของ NO ด้วย NH_3. (FORMATION OF N_2O AND SO_3 ON V-W-MO/TIO_2 CATALYSTS PREPARED FROM SEQUENTIAL LOADING METHOD DURING THE SELECTIVE REDUCTION OF NO WITH NH_3) อ.ที่ปรึกษาวิทยานิพนธ์หลัก: รศ.ดร.ธราธร มงคลศรี, 78 หน้า.

งานวิจัยนี้ทำการศึกษา การเกิด N_2O และ SO_3 บนตัวเร่งปฏิกิริยา V-W-Mo/TiO_2ซึ่งเตรียมโดยวิธีการเติมโลหะเป็นลำดับในระหว่างปฏิกิริยารีดิวซ์แบบเลือกเกิดของ NO ด้วย NH_3 การทดสอบการเกิด N_2O และ SO_3 กระทำในช่วงอุณหภูมิ 120°C-450°C พบว่าทุกตัวเร่งปฏิกิริยา V-W-MO/TiO_2 ทำให้เกิด N_2O ในช่วงอุณหภูมิสูง และเพิ่มขึ้นอย่างมีนัยสำคัญเมื่อ NO conversion ลดลง การเกิด N_2O เป็นปฏิกิริยาระหว่าง NH_3 บนพื้นผิวกับ NO ซึ่งเป็นไปตามกลไกของ Eley-Rideal และพบว่าการลดปริมาณ W ส่งผลต่อการเพิ่มขึ้นของปริมาณ N_2O แต่การลดลงของปริมาณ Mo มีผลเพียงเล็กน้อย ในส่วนของการเกิด SO_3 จากการออกซิเดชันของ SO_2 นั้นตรวจไม่พบการเกิด SO_3 จากตัวเร่งปฏิกิริยาทุกตัวที่ทำการศึกษา

ภาควิชา วิศวกรรมเคมี	ลายมือชื่อนิสิต
สาขาวิชา วิศวกรรมเคมี	ลายมือชื่อ อ.ที่ปรึกษาวิทยานิพนธ์หลัก
ปีการศึกษา 2555	

5470108421 : MAJOR CHEMICAL ENGINEERING
KEYWORDS : SELECTIVE CATALYTIC REDUCTION (SCR)/ VANADIUM OXIDE/ TUNGSTEN OXIDE/ MOLYBDENUM OXIDE /TITANIUM (IV) OXIDE/ AMMONIA/ NITRUS OXIDE/ SULFUR DIOXIDE

KAMOLTIP SAEBANG: FORMATION OF N_2O AND SO_3 ON V-W-MO/TIO_2 CATALYSTS PREPARED FROM SEQUENTIAL LOADING METHOD DURING THE SELECTIVE REDUCTION OF NO WITH NH_3. ADVISOR: ASSOC.PROF. THARATHON MONGKHONSI, Ph.D., 78 pp.

This work studies formation of N_2O and SO_3 on V-W-Mo/TiO_2 catalysts that prepared from sequential loading method during the selective catalytic reduction of NO with NH_3. The formation of N_2O and SO_3 testing is carried out in a temperature range 120°C-450°C. The results indicate that all catalysts produced N_2O at high temperature and significant increasing of N_2O when NO conversion decreases. The formation of N_2O occurs from the reaction between NH_3 on surface of catalyst and NO in gas phase followed Eley-Rideal mechanism. It also found that decreasing amount of W content tends to increases the amount of N_2O, but decreasing amount of Mo content was less affected. In the part of formation of SO_3, it is found that overall the catalysts studied, the oxidation of SO_2 to SO_3 does not occur.

Department : Chemical Engineering	Student's Signature
Field of Study : Chemical Engineering	Advisor's Signature
Academic Year : 2012	

ACKNOWLEDGEMENTS

I would like to express my sincere thanks to my thesis advisor, Assoc. Prof. Dr. Tharathon Mongkhonsi for his invaluable help and constant encouragement throughout the course of this research. I am grateful for his teaching and advice, not only the research methodologies but also many other methodologies in life. I would not have achieved this far and this thesis would not have been completed without all the support that I have always received from him.

Kietlada and in supported me so much in all research's experimental. I had a real pleasure to stay with my friends who were in Center of Excellence on Catalysis and Catalytic Reaction Engineering, Chulalongkorn University during studying: Weeranuch, Noppamas, Siwaporn, Wararee, Arpatchanee, Jitraporn, Boonwara and Pongsatorn.

In addition, I am most grateful for financial support from the PTT Public Company Limited.

Finally, I would like to dedicate the achievement of my work to my family. Without their love, support, encouragement, and understanding, I do not know if I would be able to finish this work ever.

CONTENTS

Page

CHAPTER Page

LIST OF TABLES

TABLE Page

LIST OF FIGURES

FIGURE Page

FIGURE Page

CHAPTER I

INTRODUCTION

A combined cycle of gas and steam turbines is used in the process of generating electrical power. In order to achieve high performance a high fuel combustion temperature is required, which results in nitrogen oxide (NO, NO_2 and N_2O) emission caused by oxidation of nitrogen compounds in the fuel and/or oxidation of atmospheric nitrogen in the combustion air. Emissions of NO_x cause acidification of the environment and smog formation in the atmosphere, such as acid rain, photochemical smog, ozone depletion, and greenhouse effect. NO_x can be reduced by a variety of methods. The selective catalytic reduction (SCR) of NO_x with NH_3 is one of the most efficient and widely used methods for flue gas cleaning. SCR is a process in which a reducing agent (ammonia) reacts selectively with NO_x to produce N_2 as shown in equations 1.1-1.2.

$$2NO_2 + 4NH_3 + O_2 \rightarrow 5N_2 + 6H_2O \qquad \text{(eq. 1.1)}$$

$$4NO + 4NH_3 + O_2 \rightarrow 4N_2 + 6H_2O \qquad \text{(eq. 1.2)}$$

At a high reaction temperature, the following undesirable oxidation of NH_3 to NO, N_2 and N_2O may also occur:

$$4NH_3 + 5O_2 \rightarrow 4NO + 6H_2O \qquad \text{(eq. 1.3)}$$

$$4NH_3 + 3O_2 \rightarrow 2N_2 + 6H_2O \qquad \text{(eq. 1.4)}$$

$$2NH_3 + 2O_2 \rightarrow N_2O + 3H_2O \qquad \text{(eq. 1.5)}$$

As shown in equation 1.5, N_2O (Nitrous oxide) is a byproduct of ammonia oxidation. Because N_2O is not included in the generic term for NO_x and cannot be reduced by the normal SCR process as shown in equations 1.1 and 1.2, therefore operating condition for the SCR to avoid apparent N_2O is necessary as N_2O is a powerful greenhouse gas and has been reported to destroy the ozone in the protective layer of the upper atmosphere.

In addition, if the fuel contains sulfur. The sulfur compound(s) can react with oxygen to produce $SO_{3,}$ resulting in sulfur dioxide which can be further oxidized as shown in equation 1.6.

$$2SO_2 + O_2 \rightarrow 2SO_3 \qquad \text{(eq. 1.6)}$$

SO_3 can react with unconverted NH_3, as shown in equation 1.7 and 1.8, to form ammonium bisulfate, a sticky, corrosive compound, which fouls heat exchanger and other equipment downstream of power plant.

$$2NH_3 + SO_3 + H_2O \rightarrow (NH_4)_2SO_4 \qquad \text{(eq. 1.7)}$$
$$NH_3 + SO_3 + H_2O \rightarrow NH_4HSO_4 \qquad \text{(eq. 1.8)}$$

Commercial V_2O_5/TiO_2 catalysts are very active and selective and have reasonable operating temperature windows (300-400°C), reasonably stable, resistant to poisoning by SO_2 even at high concentration. They, however, are still active for SO_2 oxidation to SO_3 when increasing vanadium oxide and increasing reaction temperature (V_2O_5 catalyst are used for sulfuric acid production at $T > 450°C$). The optimal loading of vanadium oxide on tiatania surface is most essentially. The good catalyst for SCR must be able to operate in various conditions as such the addition of a promoter is able to speed up the operation.

WO_3 and MoO_3 are the promoters of choice for the vanadia catalyst. These additives prevent the transformation of anatase to rutile, increase Brönsted acidity, blocking adsorption of SO_3. For example, V_2O_5-MoO_3/TiO_2 can remove NO_x at low temperature 150-350°C (Taweesuk, 2011) and V_2O_5-WO_3/TiO_2 can remove NO_x at high temperature 200-400°C. (Mongkhonsi and Kaewbuddee, 2012), therefore three mixed oxide (V_2O_5-WO_3-MoO_3), will be an alternative catalyst for SCR as it is will be able to remove NO_x at low and high temperature that are operating conditions temperatures of each power plant.

However, in the past, the developed catalysts for the selective catalytic reduction of NO with NH_3 were determined by efficient of removal NO, but not mention the formation of N_2O and the oxidation of SO_2. Therefore a good catalyst for the removal of NO may be not a good catalyst when considering the formation of N_2O and oxidation of SO_2.

This work is a continuation of a previous work by Kietlada Warinsirirux, 2011. The previous work has developed three mixed oxide catalyst (V_2O_5-WO_3-MoO_3/TiO_2) for the selective catalytic reduction of NO_x with NH_3.

The objective of this research is to determine the formation of N_2O and SO_3 over V_2O_5-WO_3-MoO_3/TiO_2 catalyst during the selective catalytic reduction with NH_3 process that contains high concentration of sulfur dioxide and oxygen and including H_2O at temperature ranging between 120°C and 450°C.

This research has been scoped as follows:

1. Catalytic activity testing.
   1.1 Determination of the reduction of NO with NH_3.

Feed gases composition:	120 ppm NO
	120 ppm NH_3
	15% by volume O_2
	30 ppm SO_2
	15% by volume H_2O
Total flow rate:	200 ml/min
Reaction temperature range:	120°C-450°C

1.2 Determination formation of N_2O during the selective catalytic reduction of NO with NH_3.

Feed gases composition: 120 ppm NO
120 ppm NH_3
15% by volume O_2
30 ppm SO_2
15% by volume H_2O
N_2 balanced
Total flow rate: 200 ml/min
Reaction temperature range: 120°C-450°C

1.3 Determination formation of NO from NH_3 oxidation during the selective catalytic reduction of NO with NH_3.

Feed gases composition: 120 ppm NH_3
15% by volume O_2
30 ppm SO_2
15% by volume H_2O
N_2 balanced
Total flow rate: 200 ml/min
Reaction temperature range: 120°C-450°C

1.4 Determination formation of SO_3 from SO_2 oxidation during the selective catalytic reduction of NO with NH_3.

Feed gases composition: 30 ppm SO_2
15% by volume O_2
120 ppm NO
N_2 balanced
Total flow rate: 200 ml/min
Reaction temperature range: 120°C-450°C

2. Measuring concentration of NO, N_2O and SO_2 by Shimadzu GC-2014

   2.1 Measuring concentration of NO

Detector:	Electron Capture Detector
Column:	Hyasep-DB
Temp column:	40°C

   2.2 Measuring concentration of N_2O

Detector:	Electron Capture Detector
Column:	Hyasep-DB
Temp column:	150°C

   2.3 Measuring concentration of SO_2

Detector:	Flame Photometric Detector
Column:	Rt-XL sulfur
Temp column:	180°C

The present thesis is organized as follows:

Chapter I describes background, objective and scopes of the research.

Chapter II presents principles of SCR of NO by NH_3, NH_3 oxidation, SO_2 oxidation and SCR catalysts.

Chapter III presents procedure for preparation of titania and three mixed oxide (V_2O_5-WO_3-MoO_3/TiO_2) catalyst, characterization of the catalyst and catalytic activity testing.

Chapter IV presents result of the catalytic activities testing.

Chapter V presents conclusion and recommendation of the research.

CHAPTER II

THEORY AND LITERATURE REVIEWS

This chapter presents previous studies that relate to NO_x removal technologies, the selective catalytic reduction (SCR) of nitrogen oxide (NO_x) with ammonia (NH_3) including ammonia oxidation, sulfur dioxide oxidation and SCR catalysts.

2.1 NO_x removal technologies

NO_x arises from a number of different sources, including fuel NO_x, which is formed by oxidation of nitrogen containing compounds in the fuel. Thermal NO_x,which is formed by oxidation of atmospheric nitrogen, from the combustion air. Prompt NO_x, which is formed by oxidation of intermediate species such as HCN (Bosch and Janssen, 1988). Thus, NO_x removal technologies need to have high efficiency. Table 2.1 shows the variety of methods can be reduced $NO_{x.}$ One of the most efficiency is catalytic reduction of NO_x by the selective catalytic reduction (SCR) which can be reduced NO_x reaching to 90%.

2.2 The Selective Catalytic Reduction (SCR) of NO_x with NH_3

The selective catalytic reduction (SCR) plays major role worldwide and the trend of industry power plant also pushes forward the development of new flue gas cleaning technologies. This technology can reduce nitric oxide (NO and NO_2) that is released from stationary source and using a reducing agent such as ammonia (NH_3) which reacts selectively with the NO to produce N_2. The two main reactions in the SCR process show in equation 2.1-2.2.

$$6NO + 4NH_3 \rightarrow 5N_2 + 6H_2O \quad \text{(eq. 2.1)}$$

$$4NO + 4NH_3 + O_2 \rightarrow 4N_2 + 6H_2O \quad \text{(eq. 2.2)}$$

Table 2.1 Different methods for NO_x reduction in flue gases (Gabrielsson and Pedersen, 2008).

Mechanism	Technique	Efficiency%
Reduced peak temperature	Water injection	40-70
	Flue gas recirculation	40-80
	Burner out service	30-60
	Less excess air firing (LEA)	15-20
Limiting thermal NO_x formation	Oxyfuel	70-90
Lower residence time at peak temperature	Low-NO_x burners, overfire air, staged combustion, rotating opposed fired air, etc.	30-70
Catalytic reduction of NO_x	Selective catalytic reduction (SCR)	70-98
	Selective non-catalytic reduction (SNCR)	25-50
	Adsorption and reduction NO_x	60-90

Equations 2.1 and 2.2 are the SCR reaction of NO with NH_3. Both equations can convert NO to N_2. It is known that nitrogen oxides (NO_x) also contains NO_2, NO_2 can react with NH_3 as showed in equation 2.3 below

$$2NO_2 + 4NH_3 + O_2 \rightarrow 3N_2 + 6H_2O \qquad \text{(eq. 2.3)}$$

Selective reduction of NO and NO_2 with NH_3 occurs with high activity and selective to N_2 within a narrow temperature window of 50-150°C. This window typically occurs within the broad temperature range of 150-500°C. The precise location is catalyst-dependent.

2.3 The ammonia (NH_3) oxidation

NH_3 is supplied to SCR process using the gaseous (anhydrous form), an aqueous solution, or a solution of urea. The choice will depend on economy and any safety issue involved in handling the most preferred anhydrous ammonia (Gabrielsson and Pedersen, 2008). Due to the SCR of NO_x used ammonia as a reducer, in case of the feed gases includes excess O_2 and high temperatures may be occurs the ammonia oxidation which side reaction are undesirable.

The ammonia oxidation is the side reaction when NH_3 reacts with excess O_2 at high temperatures. It is a main side reaction of the SCR because it produces NO and N_2O. The different stoichiometric reactions of ammonia oxidation are show in equation 2.4-2.6.

$$4NH_3 + 5O_2 \rightarrow 4NO + 6H_2O \qquad \text{(eq. 2.4)}$$

$$2NH_3 + 2O_2 \rightarrow N_2O + 3H_2O \qquad \text{(eq. 2.5)}$$

When NH_3 oxidation occurs in parallel with the SCR reaction, NH_3 consumption is greater, while NO_x removal efficiency is lower. Since the rates of the oxidation reactions are generally more temperature sensitive than NO reduction, their competition is greater at higher reaction temperatures, leading to a decrease in net NO_x conversion. Accordingly, there was a window for high conversions of NO_x, reaching a maximum at medium reaction temperatures. (Bartholomew and Farrauto, 2010)

Formation of nitrous oxide (N_2O) is according to equation 2.5. N_2O cannot be reduced by normal SCR process and not included in the generic term for NO_x (Gabrielsson and Pedersen, 2008). It is, however, a powerful greenhouse gas (i.e. it absorbs the sun’s infrared energy) and has been reported to destroy the ozone in the protective layer of the upper atmosphere. (Stratospheric ozone absorbs, through a cycle of reactions, the sun’s damaging UV rays, which would otherwise reach the earth’s surface.) (Bartholomew and Farrauto, 2010)

2.4 The sulfur dioxide (SO_2) oxidation

Sulfur dioxide can reacts with oxygen to form sulfur trioxide as showed in equation 2.6. SO_3 ultimately react with unconverted NH_3 to form ammonium bisulfate according to equation 2.6, a sticky, corrosive compound, which fouls heat exchangers and other equipment downstream.

$$2SO_2 + O_2 \rightarrow 2SO_3 \quad \text{(eq. 2.6)}$$

$$2NH_3 + SO_3 + H_2O \rightarrow (NH_4)_2SO_4 \quad \text{(eq. 2.7)}$$

$$NH_3 + SO_3 + H_2O \rightarrow NH_4HSO_4 \quad \text{(eq. 2.8)}$$

SO_2 oxidation increased almost linearly with V_2O_5 loading below the monolayer capacity and attained saturation with further increase (Kamata et al, 2001). Sulfation occurs when commercial vanadia SCR catalysts are exposed to SO_2-laden coal combustion flue. It can inhibit NO adsorption in the presence of oxygen, but greatly enhances NH_3 adsorption by generating additional Brönsted acid sites while reducing the concentration of Lewis acid sites. (Guo et al, 2009)

2.5 SCR catalyst

The main requirements for an SCR catalyst includes, high volume activity for remove NO, low sulfur oxidation activity, high mechanical or attrition strength, high deactivation resistance and low price (Gabrielsson and Pedersen, 2008). selective catalytic reduction of NO_x with NH_3 is partial oxidation reaction required catalyst in form oxides phase such as vanadium oxide (V_2O_5), molybdenum oxide (MoO_3), tungsten oxide WO_3 and copper oxide CuO.

The choice of support material is also dependent on the activity with active ingredients and its stability. It is possible to obtain good SCR activities in the industrial temperature window with alumina (Al_2O_3), zirconia (ZrO_2), and titania (TiO_2).

- Alumina (Al_2O_3) are the most common commercial carriers because of their excellence thermal stability and wide range of chemical, physical and catalytic properties but it easy to sulfate.
- Titania (TiO_2) has found limited application, as a support for vanadia catalyst used in NO_x, Commercial high surface area titanias (25-100 m^2/g) are formed by precipitation from titanate solutions or by decomposition of organotitanates, although new preparations from the aerogel promise to provide materials of higher surface area (200-400 m^2/g). In general, commercial titanias consist of 2 phases or crystal structures: anatase and rutile.
    - Anatase is the most important catalytically. in that it has a surface area of about 50-80 m^2/g.
    - Rutile structure forms at about 500 °C and low surface area.

Essentially, the transformation of anatase to rutile generally results in surface area loss. Only titania exhibits a sulfur tolerance, which is sufficient for the industrial high-temperature application while alumina and zirconia are rather easy to sulfate, which might affect their activity and mechanical stability. As such a TiO_2 is the good support choice for SCR process. It can be by various methods prepared various methods such as sol-gel, solvothermal and flame spray pyrolysis. The favorite method is sol-gel because it has mild condition (low temperature and ambient pressure), high purity precise stoichiometry, controllable pore size and porosity and no special equipment.

2.6 The surveys of previous studies for SCR catalysts

The first catalyst for SCR, Pt and Pd were developed in the early 1970s. While they were very active for NO reduction at 125-175°C, they are also active for the oxidation of NH_3 and SO_2 when reaction temperature is above 200°C and also less tolerant to poisoning and undesirably selective for N_2O.

Among metal oxides catalyst, investigated since the mid-1960s, V_2O_5/TiO_2 catalyst promoted with WO_3 or MoO_3 were found to be the most effective and the dominant SCR catalysts technology from about 1980 to the present. Although V_2O_5/TiO_2 catalyst is less active than Pt but V_2O_5/TiO_2 has higher and larger operating temperature window (300-400°C). (Bartholomew and Farrauto, 2010)

Zeolite have ideal properties for SCR, i.e. high acid site concentration, high surface area, high thermal stability, permit operation at much higher temperatures and over windows (350-500°C) and advantage for some turbine applications since less cooling is required, but they are the less active and significantly more expensive than V_2O_5/TiO_2 catalysts. (Bartholomew and Farrauto, 2010)

V_2O_5/TiO_2 catalyst, however, is the technology of choice for NO_x abatement in large power plants because its operating temperature is a good match to the flue gas temperature at the exit of economizer and its cost relative to either Pt or zeolite catalysts is significantly lower. They are very active and selective, reasonably stable in the presence of coal ash, resistant to poisoning by SO_2 even at high concentrations and operate near the ideal temperature range of 300-400°. Unfortunately these catalyst are active for SO_2 oxidation to SO_3 and since SO_2 concentration is high at this location, catalyst activity is purposely limited to prevent this reaction and subsequent downstream corrosion/-fouling of heat exchangers by ammonium sulfates formed by reaction of SO_3 and NH_3 and due to costs for handling and disposing of spent catalyst are high. In order to avoid SO_2 oxidation, optimize level of vanadium depending on the support was about 3% w/w (Amiridis et.al, 1996)

The promoters for the vanadium and titanium-based catalyst that exhibited the highest number of Brönsted acid sites, and which exhibited the highest SCR activity, were the metal oxides WO_3 and MoO_3, which are commonly used in industrial catalyst today. WO_3 is employed in larger amount 10%w/w (Chen and yang, 1992). It acts both as chemical and structural promoter by enlarging the temperature window of the SCR reaction and by improving the mechanical, structural and morphological properties of the catalysts. MoO_3 (loadings as high as 6% w/w) has been reported to be less active than V_2O5-WO_3/TiO_2 but more tolerant to As.

V_2O_5-WO_3/TiO_2 catalysts are co-oxide catalyst which added WO_3 to V_2O_5/TiO_2. These catalysts were reported to be more active than V_2O_5/TiO_2 (Casagrande et.al, 1999) wanted removed NO_x at high temperature (200°C-400°C) (Mongkhonsi and kaewbuddee, 2012), Similarly V_2O_5-MoO_3/TiO_2 catalysts are co-oxide catalyst which added MoO_3 to V_2O_5/TiO_2. These catalysts can remove NO_x at low temperature (150°C-350°C) (Taweesuk, 2010)

V_2O_5-WO_3-MoO_3/TiO_2 catalysts are three mixed oxide over titania support. In order to improved Co-Oxide catalyst for good performances at high temperature (above 200°C) and give high NO conversion in wide reaction temperature range. (Warinsirirux, 2011) and the suitable composition of these catalyst was 3%V, 7%W, 5%Mo very active to removed NO_x in wide rang temperature. (Piyanantarak, 2011)

2.7 Comment on the previous work

In the previous work, good method for removal NO_x is the selective catalytic reduction with NH_3. The suitable catalyst for SCR is V_2O_5-WO_3-MoO_3/TiO_2 (three mixed oxide). It has high efficiency to remove NO_x and reaching to 80-100% (Warinsirirux, 2011). However, the selective catalytic reduction process appears the main side reaction for instant sulfur dioxide oxidation and ammonia oxidation therefore formation of N_2O and SO_3 are necessary to measure.

Generally, selective catalytic reduction of NO_x with NH_3 describes especially net NO reduction conversion and feed gases compose NO, NH_3, O_2 (without SO_2 and H_2O) for example, the research of Nova and others (1998), Boyano and others (2009) Haitao and others (2010) (see table 2.2). Although, in case of flue gases compose high concentration of O_2 and appearance of SO_2 and H_2O was previously studied by Warinsirirux, 2011 and Piyanantarak, 2011 only NO conversion was measured. There is no study on the formation of N_2O and the oxidation of SO_2 to SO_3.

In the previous research the V_2O_5-WO_3-MoO_3/TiO_2 catalyst been shown to have high performance for NO_x removal but the formation of N_2O and SO_3 that may be occur in this system at high concentration of O_2, H_2O and SO_2 (15%O_2, 15%H_2O and 30 ppm SO_2) was not mentioned. Thus the purpose of this research is to determine the formation of N_2O and SO_3 during the SCR process of the V_2O_5-WO_3-MoO_3/TiO_2 catalysts that mention in the previous research (Warisirirux, 2011).

Table 2.2 The surveys of catalysts and operating condition for SCR.

Year	Researcher	Catalyst	Temp(°C)	Feed gases composition						Measuring
				NO(ppm)	NH_3(ppm)	O_2(%vol)	SO_2(%vol)	H_2O(%vol)	balanced	
1998	Beretta et.al	V/TiO_2 $V/Mo/TiO_2$ $V/W/TiO_2$	380	500	550	2	500	10	N_2	NO_X, SO_2
1998	Nova et.al	WO_3/TiO_2	550	800	800	9000 ppm	-	-	He	NO
1998	Orsenigo et.al	V_2O_5-WO_3/TiO_2	330 - 380	500	550	2	500	10	N_2	NO, SO_3
1999	Casagrande et.al	V_2O_5-WO_3/TiO_2	27-527	800	800	9000 ppm	-	-	He	NO, N_2O
1999	Delahay et.al	Cu-FAU	80-450	2000	2000	3	-	-	N_2	NO, N_2O
2001	Kamata et.al	V_2O_5/TiO_2	300-460	-	-	7500 ppm	500	-	N_2	SO_2
2002	Huang et.al	V_2O_5/AC	250	500	600	3.4	2.5	500	Ar	NO, SO_2
2002	Jung et.al	V_2O_5	100-400	0.1	0.105	2.5	-	-	He	NO, N_2O
2003	Qi and Yang	Fe-Mn/TiO_2	80-180	1000	1000	2	100	2.5	He	NO
2009	Boyano et.al	V_2O_5/AC V_2O_5/Al_2O_3	150-350	1000	1000	10	-	-	Ar	NO
2010	Haitao et.al	Si-Ce complex oxide	100-500	600	600	5	-	-	N_2	NO

Table 2.2 The surveys of catalysts and operating condition for SCR. (con,t)

year	Researcher	Catalyst	Temp(°C)	Feed gases composition						Measuring
				NO(ppm)	NH_3(ppm)	O_2(%vol)	SO_2(%vol)	H_2O(%vol)	balanced	
2010	Gao et.al	CeO_2-TiO_2	150-450	1000	1000	3	200 ppm	10	N_2	NO
2010	Shen et.al	Iron-droped Mn-Ce/TiO_2	80-260	0.06%	0.06%	3	0.01	3	N_2	NO, NO_2, SO_2
2010	Xiaodong et.al	MnO_x-TiO_2 CeO_2-MnO_x-TiO_2 V_2O_5-MnO_x-TiO_2	25-400	500	500	5	-	-	N_2	NO ,NO_2, N_2O, NH_3
2011	Chen et.al	Alkalai metals doping over nano V_2O_5-WO_3/TiO_2	150-500	500	500	3	-	-	N_2	NO, N_2O
2012	Xu et.al	MnO_x-CeO_2/WO_3-ZrO_2 monolith	100-450	0.1%	0.1%	5	0.01	10	Ar	NO, NH_3
2012	Lee et.al	V/TiO_2 W/TiO_2	350-450	400	420	8	-	6	Ar	NO_x

CHAPTER III

EXPERIMENTAL

This chapter shows experimental details, which can be divided into three separate procedures according to their state. The first section (3.1) is catalysts preparation. The second section (3.2) is characterization of the catalysts of the previous research. (Warinsirirux, 2011) and the last section (3.3) is procedure of catalytic activities testing (3.3).

3.1 Catalyst preparation

This section shows the detail of catalyst preparation for V_2O_5-WO_3-MoO_3/TiO_2 catalysts that were reported in Warinsirirux's thesis. The catalysts were prepared by impregnation method. Sequence of metals loading and calcinations are different. The chemicals and procedure of catalyst preparation are described below.

3.1.1 Chemicals

The chemicals used to prepare V_2O_5-WO_3-MoO_3/TiO_2 catalysts are listed in table 3.1.

Table 3.1 Chemicals used in the catalyst preparation.

Chemical	Supplier
Titanium (IV) isopropoxide, 97%	Aldrich
Ammonium metavanadate, 99.99%	Aldrich
Ammonium metatungstate hydrate, 99.99%	Aldrich
Ammonium molybdenate tetrahydrate, ≥99.0%	Aldrich
Nitric acid 65%	Aldrich
Oxalic acid hydrate	Fluka

3.1.2 Preparation of TiO_2 (anatase) by a sol-gel method

Titania-anatase (TiO_2) is prepared by a sol-gel method. In this experiment, 83.5 ml of titanium isopropoxide, used as a precursor, is added into 1000 ml of distilled water, which is mixed with 7.5 ml of nitric acid and then stirred for 3 days, or until it has a clear sol. Then the solution was dialyzed with adjusting the pH to approximately 3.5 and then subsequently dried at 110°C for 24 hours before being crushed, grinded, and calcined in air at 350°C for 2 hours.

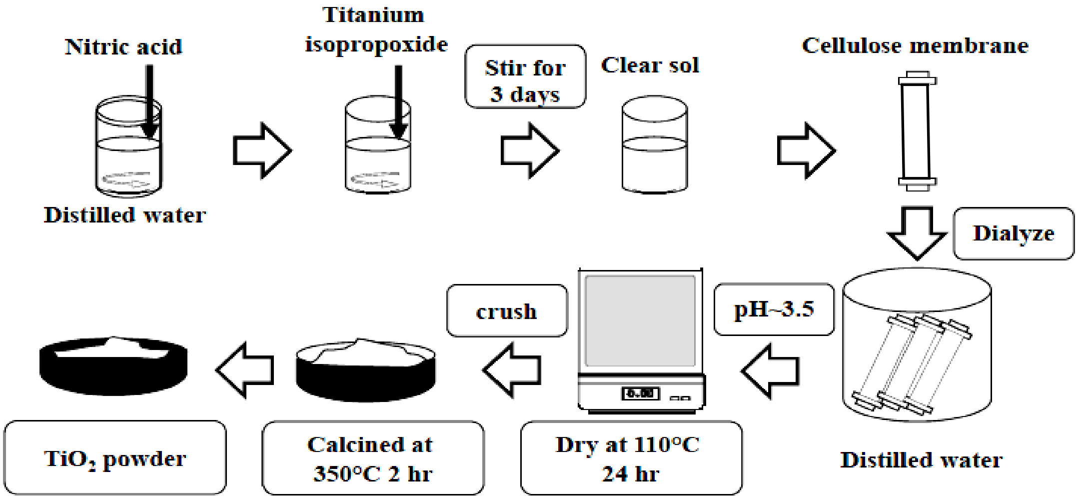

Figure 3.1 Preparation of TiO_2 by sol-gel method

3.1.3 Preparation of V_2O_5 over TiO_2 catalyst

V_2O_5 over TiO_2 catalyst is prepared by incipient wetness method. First, Ammonium metavanadate is dissolved with oxalic acid anhydrous in deionized water by a fixed amount of vanadium metal into TiO_2 approximately 3% (The volume of prepared solution is equal to the pore volume of TiO_2 powder). An ammonium metavanadate solution is obtained. Next, the prepared solution is gradually dropped into the TiO_2 powder. After that, incipient wetness point is observed. In this step a pore of TiO_2 saturated with ammonium metavanadate solution is obtained. This is then dried at 110°C for 24 hours and finally calcined in air at 500°C for 2 hours.

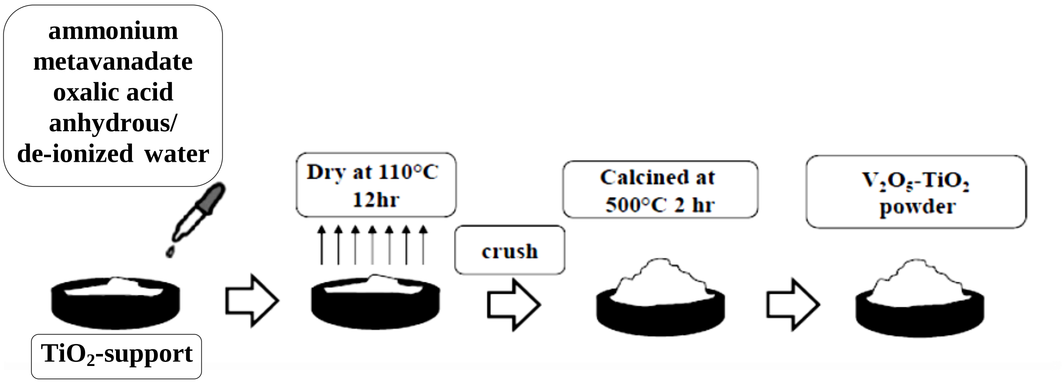

Figure 3.2 Preparation of V_2O_5/TiO_2 by impregnation method.

3.1.4 Addition of WO_3 and MoO_3 over V_2O_5/TiO_2 catalyst

Ammonium metamolybdenate tetrahydrate and ammonium metatungstate hydrate are precursors used to the promoter that are molybdenum and tungsten, are impregnated over V_2O_5/TiO_2 catalyst. The sequence of loading ammonium metamolybdenate tetrahydrate and ammonium metatungstate hydrate differs and is divided into the following three methods. See the example of calculation for the catalyst preparation in Appendix B.

3.1.5 Preparation of WO_3 and MoO_3 over V_2O_5/TiO_2 catalyst Method I

First, ammonium metatungstate hydrate is dissolved in de-ionized water, from which we obtain an ammonium metatungstate solution. Then the prepared solution is gradually dropped into the V_2O_5/TiO_2, observing the incipient wetness point. In this step a pore of V_2O_5/TiO_2 saturated with ammonium metatungstate solution is obtained. This is then dried at 110°C for 24 hours before being crushed, grinded and then calcined in air at 500°C for 2 hours. After that, ammonium metamolybdenate tetrahydrate is dissolved in de-ionized water from which we obtain an ammonium metamolybdenate tetrahydrate solution. The prepared solution is then gradually dropped into the V_2O_5-WO_3/TiO_2 observing the incipient wetness point. In this step a pore of V_2O_5-WO_3/TiO_2 saturated with an ammonium metatungstate hydrate solution is obtained. Finally it is dried at 110°C for 24 hours before being crushed, grinded and then calcined in air at 500°C for 2 hours. The sequence diagram of experiment for loading the metal is showed below:

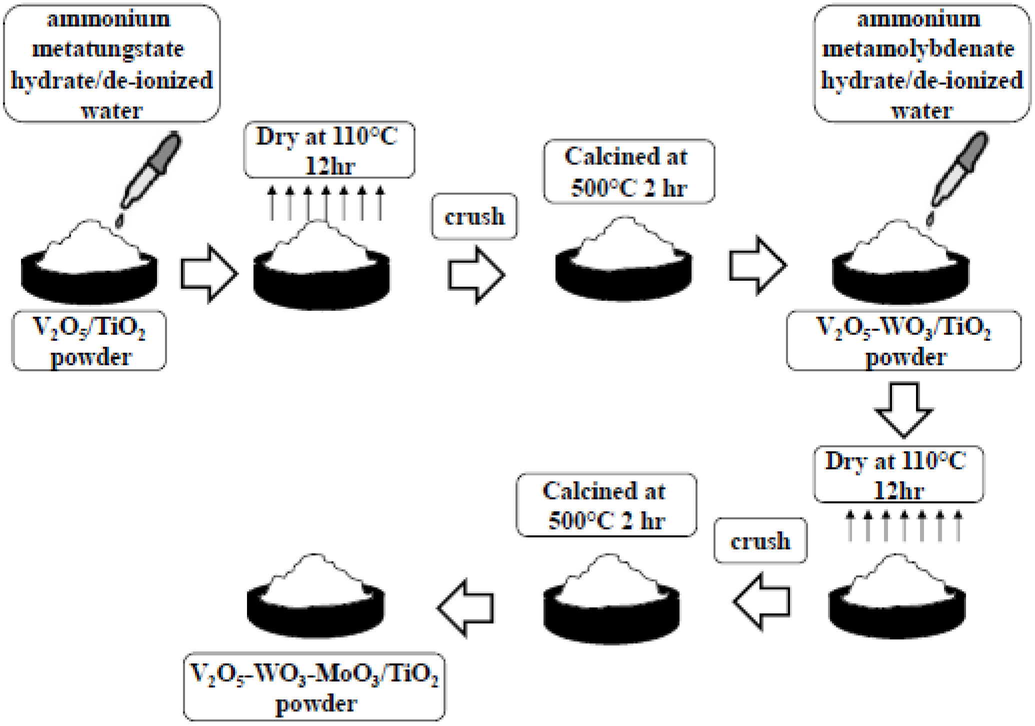

Figure 3.3 The sequence of loading metal and calcinations Method I.

3.1.6 Preparation of WO_3 and MoO_3 over V_2O_5/TiO_2 catalyst Method II

First, ammonium metamolybdenate tetrahydrate is dissolved in de-ionized water, from which we obtain an ammonium metamolybdenate tetrahydrate solution. The prepared solution is then gradually dropped into the V_2O_5/TiO_2, observing the incipient wetness point. In this step a pore of V_2O_5/TiO_2 saturated with an ammonium metamolybdenate tetrahydrate solution is obtained. This is then dried at 110°C for 24 hours before being crushed, grinded and then calcined in air at 500°C for 2 hours. After that, ammonium metatungstate hydrate is dissolved in de-ionized water. We obtain ammonium metamolybdenate tetrahydrate solution, which is gradually dropped into the V_2O_5-WO_3/TiO_2 observing the incipient wetness point. In this step a pore of V_2O_5-MoO_3/TiO_2 saturated with ammonium metatungstate solution is obtained.

Finally, this is dried at 110°C for 24 hours before being crushed, grinded and then calcined in air at 500°C for 2 hours. The sequence diagram of experiment for loading the metal is as below:

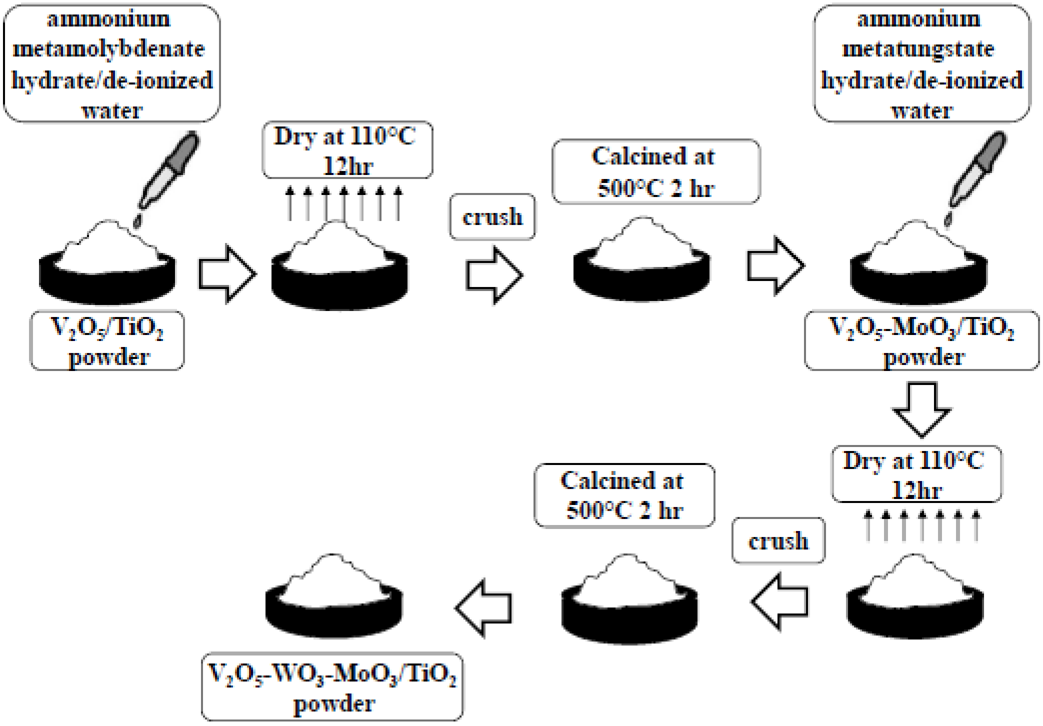

Figure 3.4 The sequence of loading metal and calcinations Method II.

3.1.7 Preparation of WO_3 and MoO_3 over V_2O_5/TiO_2 catalyst Method III

First, ammonium metatungstate hydrate and ammonium metamolybdenate tetrahydrate is dissolved in de-ionized water, from which a mixed solution of ammonium metatungstate and ammonium metamolybdenate thetrahydrate solution is obtained. The prepared solution is then gradually dropped into the V_2O_5/TiO_2, observing the incipient wetness point. In this step a pore of V_2O_5/TiO_2 saturated with mixed solution of ammonium metatungstate hydrate and ammonium metamolybdenate tetrahydrate is obtained. This is then dried at 110°C for 24 hours before being crushed, grinded and finally calcined in air at 500°C for 2 hours.

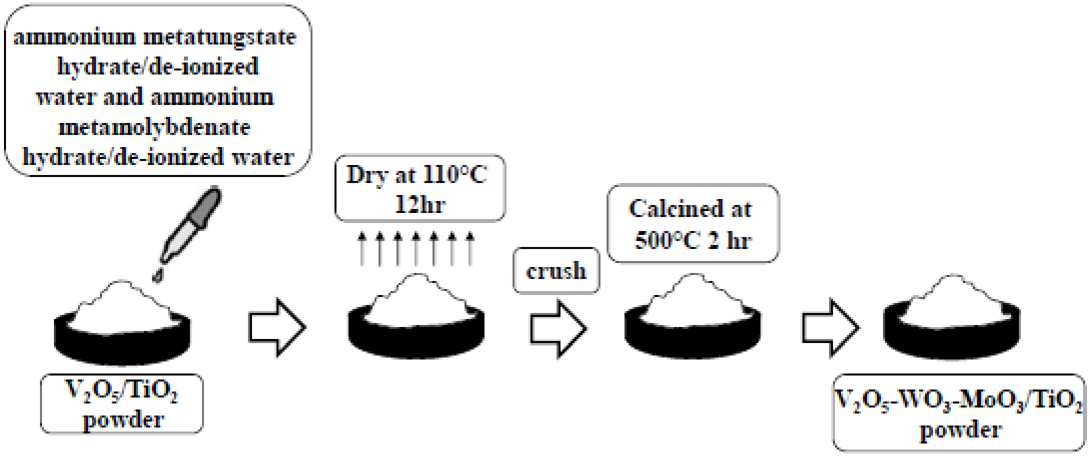

Figure 3.5 The sequence of loading metal and calcinations Method III.

3.2 Characterization of the catalysts

All the prepared catalysts were characterized in order to describe chemical and physical properties. Characterization in this experiment includes:

Inductively Coupled Plasma-Optical Emission Spectroscopy (ICP-OES) to determine percentage composition of the catalysts.

BET surface area measurement to determine specific surface area of the catalysts.

NH_3 Temperature Programmed Desorption (NH_3-TPD) to determine the amount of acid site of the catalysts

Three techniques were used to determine the V_2O_5-WO_3-MoO_3/TiO_2 catalysts by Warinsirirux, 2010. The properties of these catalysts with these techniques were shown again in this chapter. Other techniques for instant X-Ray Diffraction (XRD) and Fourier Transforms Infrared (FT-IR) were learning more in this research.

3.2.1 Inductively Coupled Plasma-Optical Emission Spectroscopy (ICP- OES)

The chemical composition percentage of all the prepared catalysts (combination of chemical elements, as active species and promoter) will be analyzed by Inductively Coupled Plasma Atomic Emission Spectrometer (ICP-AES) Perkin Elmer model PLASMA-1000. The preparation procedures of analyzed samples were as follows: First 0.2 g of the catalyst was dissolved in 10 ml of hydrofluoric (HF) 49%. Then this was stirred until it forms a homogeneous solution. The volume was then adjusted to 100 ml with a volumetric flask. The obtained concentrations of samples were about 1-24 ppm (mg/l). The result of characterization by ICP-OES shows in table 3.2.

Table 3.2 The percentage compositions of vanadium, tungsten and molybdenum on V_2O_5-WO_3-MoO_3/TiO_2 catalysts**.** (Warinsirirux, 2011)

Method	Vanadium oxide (%wt)	Tungsten oxide (%wt)	Molybdenum oxide (%wt)	Total (%wt)	Catalyst Name
I	3.2	7.2	10.5	30.9	3V7W10Mo#1
II	3.2	6.9	10.6	30.7	3V7W10Mo#2
III	3.3	7.8	10.7	31.7	3V7W10Mo#3
II	3.1	7.4	5.3	15.8	3V7W5Mo#2
II	3.1	3.4	10.3	16.8	3V3.5W10Mo#2
II	3.3	3.8	5.7	12.8	3V3.5W5Mo#2

3.2.2 BET surface area measurement

The surface area of catalyst was determined by BET surface area technique, using Micromeritrics ASAP 2020 with nitrogen as the adsorbate. The sample cell contained 0.2 g of sample and the operating condition was set to 200°C. The specific surface area of the V_2O_5-WO_3-MoO_3/TiO_2 catalysts are showed in table 3.3.

Table 3.3 The specific surface area of V_2O_5-WO_3-MoO_3/TiO_2 catalysts and TiO_2 support. (Warinsirirux, 2011)

Catalyst Sample	**BET surface area (m^2/g)**
TiO_2	90.9
3V7W10Mo#1	39.1
3V7W10Mo#2	43.7
3V7W10Mo#3	40.2
3V7W5Mo#2	44.0
3V3.5W10Mo#2	45.2
3V3.5W5Mo#2	47.8

From table 3.3, the specific surface areas of the catalysts are lower than TiO_2-support because these catalysts were passed calcinations in several time lead to aggregation of pore and losing surface area. The 3V7W10Mo#2 (prepared by method II) has specific surface area higher than 3V7W10Mo#1 and 3V7W10Mo#3 that prepared by method I and method III respectively because total percentage composition loading of 3V7W10Mo#1 and 3V7W10Mo#3 more than 3V7W10Mo#2 (see in table 3.2), so volume of pore are loss result in losing surface area.

In addition, the specific surface area of the catalysts was increased when the percentage of metal loading decreased, example 3V7W10Mo#2 (10%Mo) has specific surface area higher than 3V7W5Mo#2 (5%Mo) because percentage of molybdenum loading is lower.

3.2.3 NH_3 Temperature Programmed Desorption (NH_3-TPD)

Ammonia temperature program desorption (NH_3-TPD) is one of the most widely use and flexible techniques for characterizing the acid site on oxide surface. Determining the quantity and strength of the acid sites on catalyst surfaces and predicting the performance of a catalyst. The amount of NH_3 desorbed relates to the amount of acid site on catalyst surface and calculate from area under the curve are listed in figures 3.6-3.12 and table 3.4.

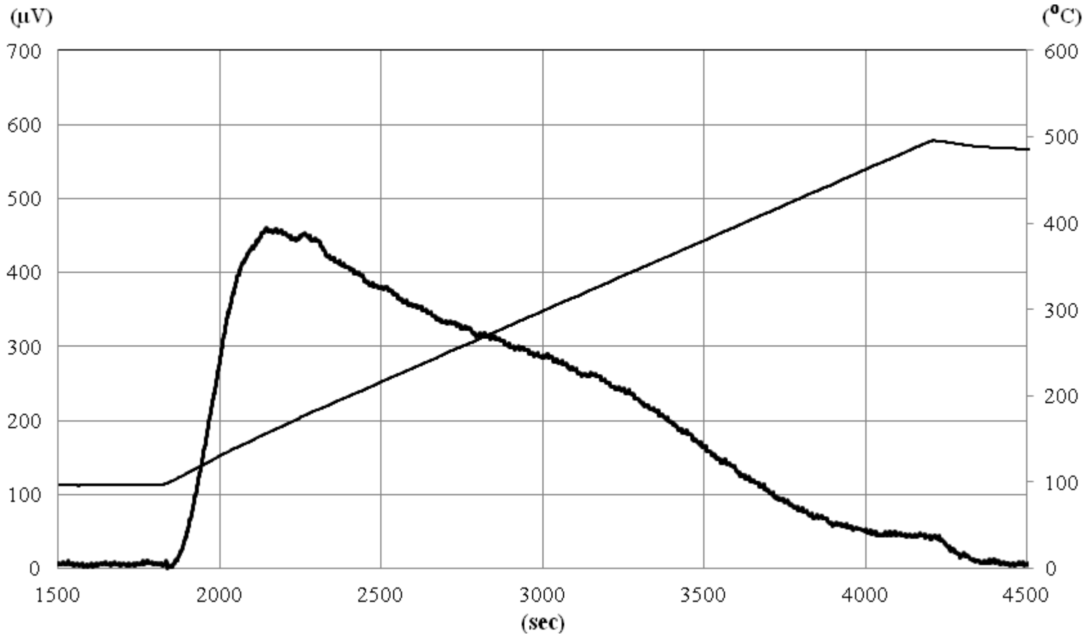

Figure 3.6 NH_3-TPD profiles of TiO_2 support. (Warinsirirux, 2011)

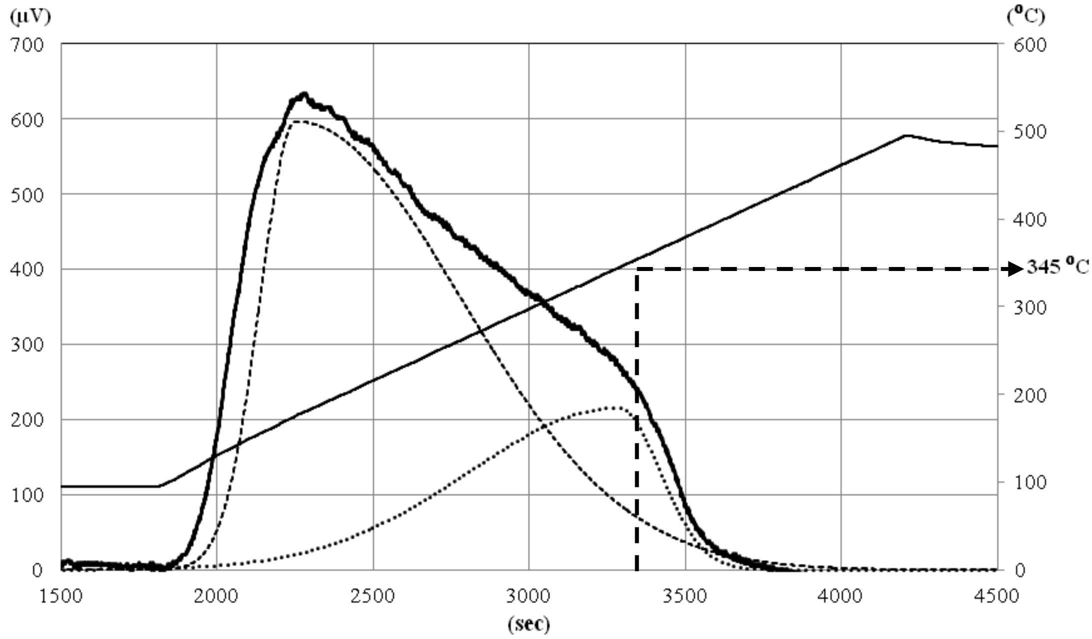

Figure 3.7 NH_3-TPD profiles of 3V7W10Mo#1 catalyst. (Warinsirirux, 2011)

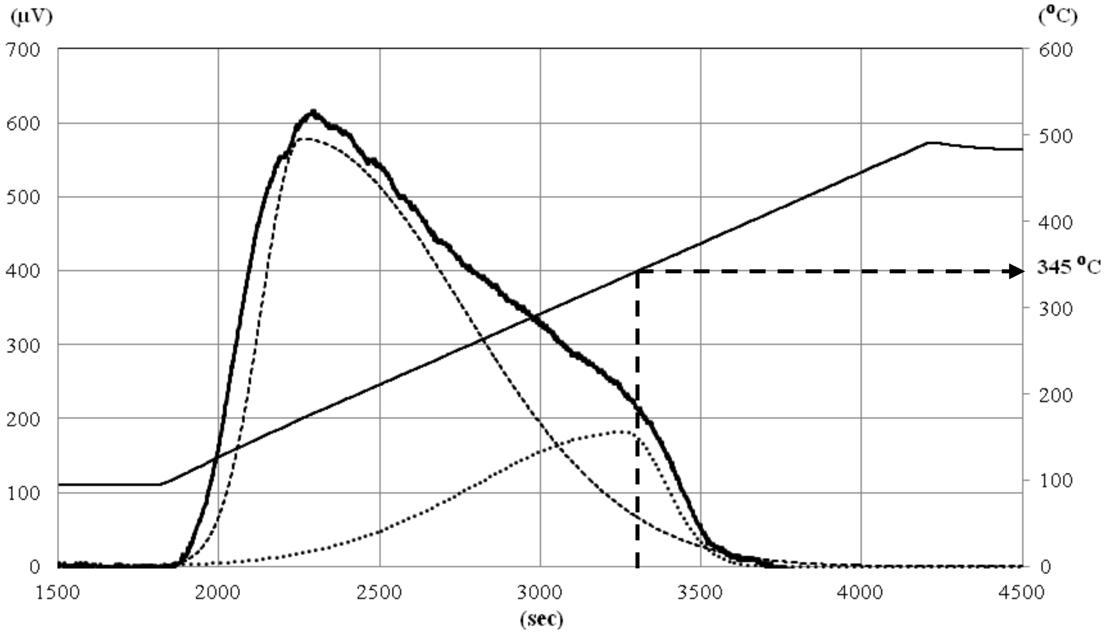

Figure 3.8 NH_3-TPD profiles of 3V7W10Mo#2 catalyst. (Warinsirirux, 2011)

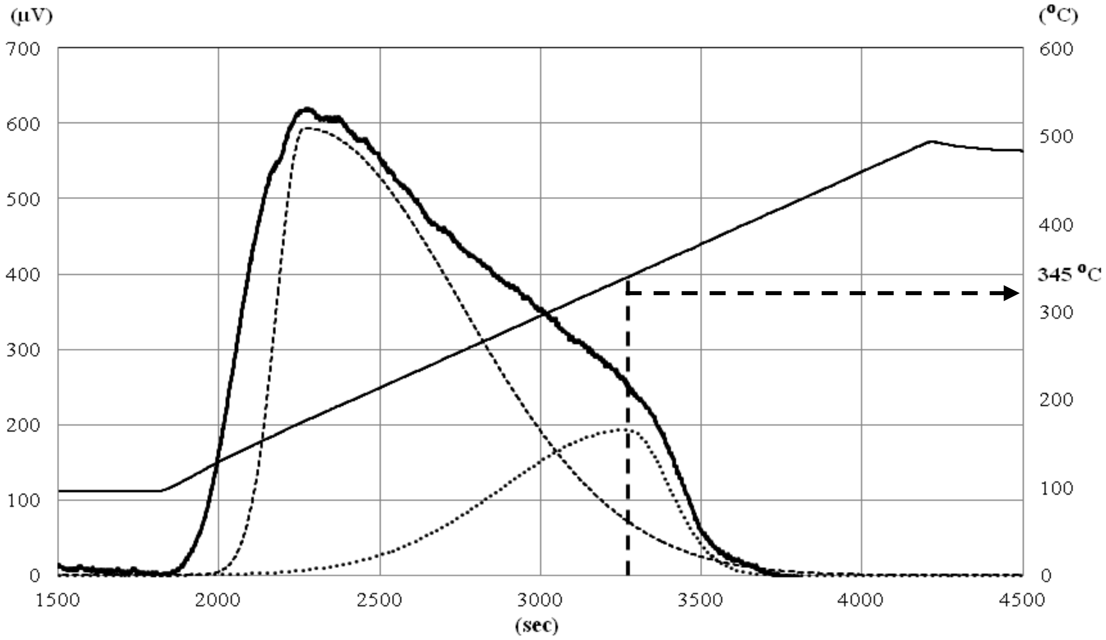

Figure 3.9 NH$_3$-TPD profiles of 3V7W10Mo#3 catalyst. (Warinsirirux, 2011)

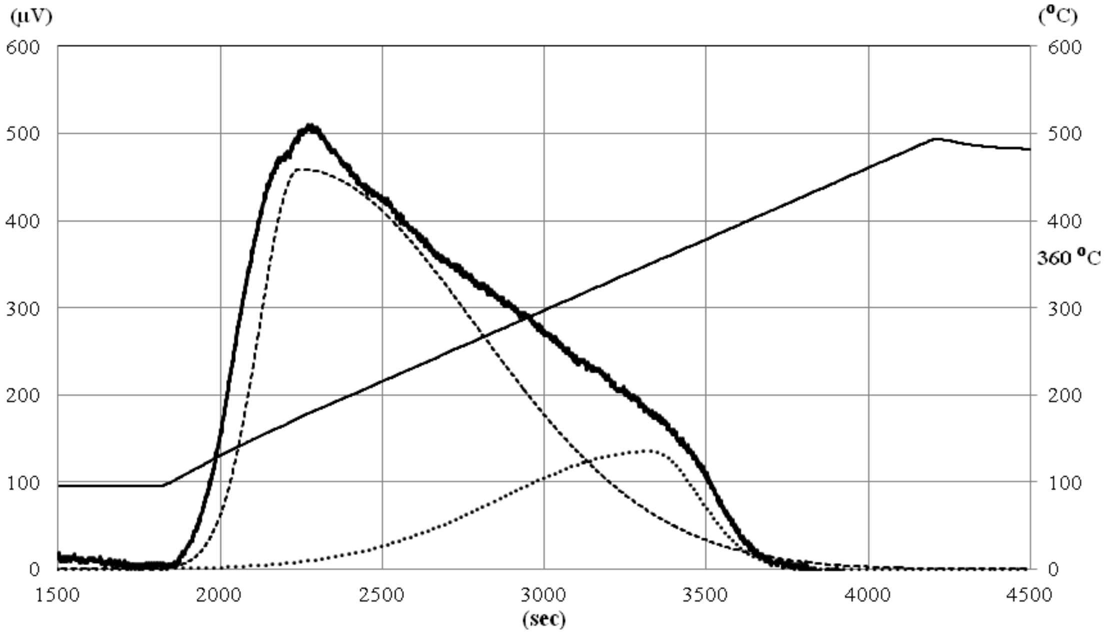

Figure 3.10 NH$_3$-TPD profiles of 3V7W5Mo#2 catalyst. (Warinsirirux, 2011)

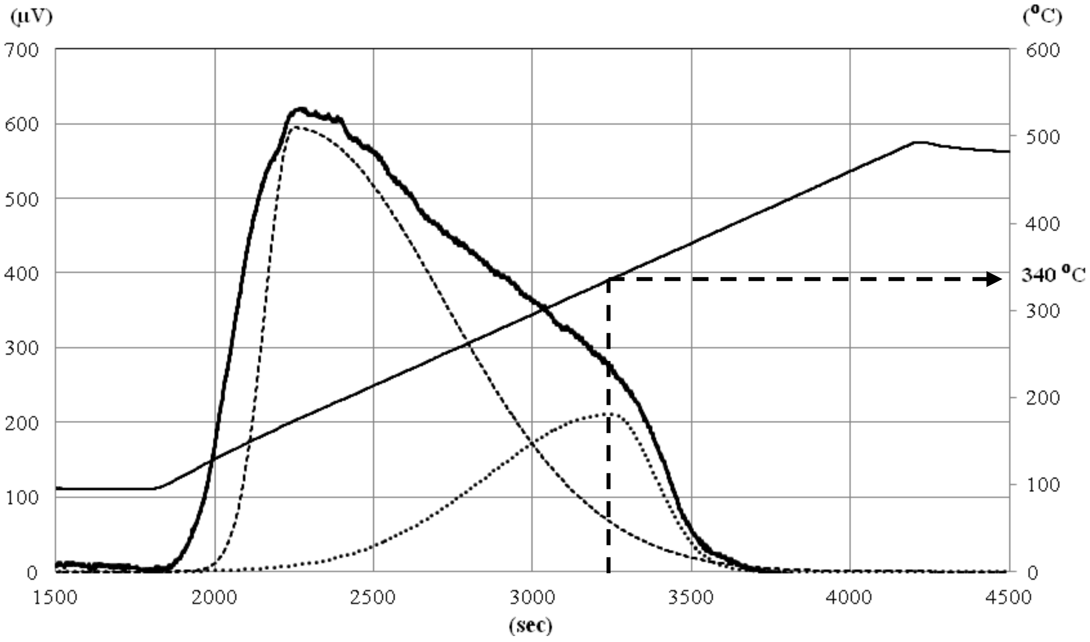

Figure 3.11 NH_3-TPD profiles of 3V3.5W10Mo#2 catalyst. (Warinsirirux, 2011)

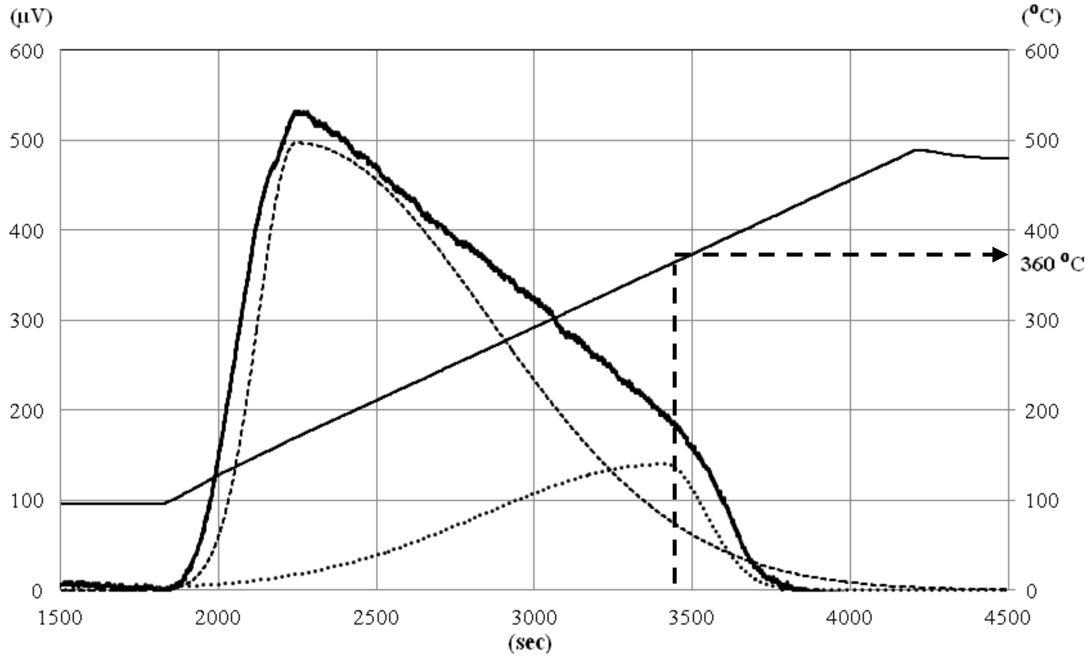

Figure 3.12 NH_3-TPD profiles of 3V3.5W5Mo #2 catalyst. (Warinsirirux, 2011)

Figures 3.6–3.12 show NH_3-TPD profiles of V_2O_5-WO_3-MoO_3/TiO_2 catalysts including TiO_2 support. The amounts of acid site were calculated from the area under the curve of desorption. The results show the two peaks of NH_3-TPD profiles of the catalysts. The first peak was found in all figures but the second peak was not found in the NH_3-TPD profile of TiO_2 support. The second peak shows the strong acid sites. Considering the amount of acid strength of these catalysts is necessary and relate to SCR reaction.

Table 3.4 The amount acid site on V_2O_5-WO_3-MoO_3/TiO_2 catalysts and TiO_2-support.(Warinsirirux, 2011)

Catalyst name	Amounts of acid site (μmolH$^+$ /g)	Amounts of strong acid site (μmolH$^+$ /g)
TiO_2	377	-
3V7W10Mo#1	378	94
3V7W10Mo#2	385	91
3V7W10Mo#3	380	88
3V7W5Mo#2	388	78
3V3.5W10Mo#2	390	87
3V3.5W5Mo#2	379	78

Although V_2O_5-WO_3-MoO_3/TiO_2 catalysts have specific surface area lower TiO_2 support, they have the same number of surface acid site see in table 3.4, This means that the addition of V, W and Mo cause losing surface area in contrast the this addition increase the acid sites on the catalysts surface.

3.2.4 X-Ray Diffraction (XRD)

The crystalline, crystalline size and crystalline pattern of the prepared catalysts are analyzed by using D8 Advance of Bruker AXS. A material that is sufficiently crystalline to diffract X-Rays (crystallites larger than 3-5 nm) is needed for characterization using this technique. The experiment is carried out by using CuKα radiation. Scans are performed over the 2Θ ranges from 20^o to 80^o with step size 0.02^o/sec and slit width 0.6 nm. The XRD spectrum is used to identify the crystal structure of the catalyst.

The XRD patterns of the V_2O_5-WO_3-MoO_3/TiO_2 catalysts that compared with TiO_2-support are displayed in Figures 3.13, the TiO_2 contained anatase phase and small amount of rutile and brookite phases. Like, the SCR catalysts, the result indicates that these catalysts pattern are same TiO_2 primary. In addition, no peak of V_2O_5, WO_3 and MoO_3 in any XRD patterns although various loading of WO_3 and MoO_3 content. However, the disappearance of other compound apart from TiO_2 on XRD pattern indicates that V, W and Mo may not form a crystal structure, but they may be form oxide structures having crystal size too small to be detected by XRD.

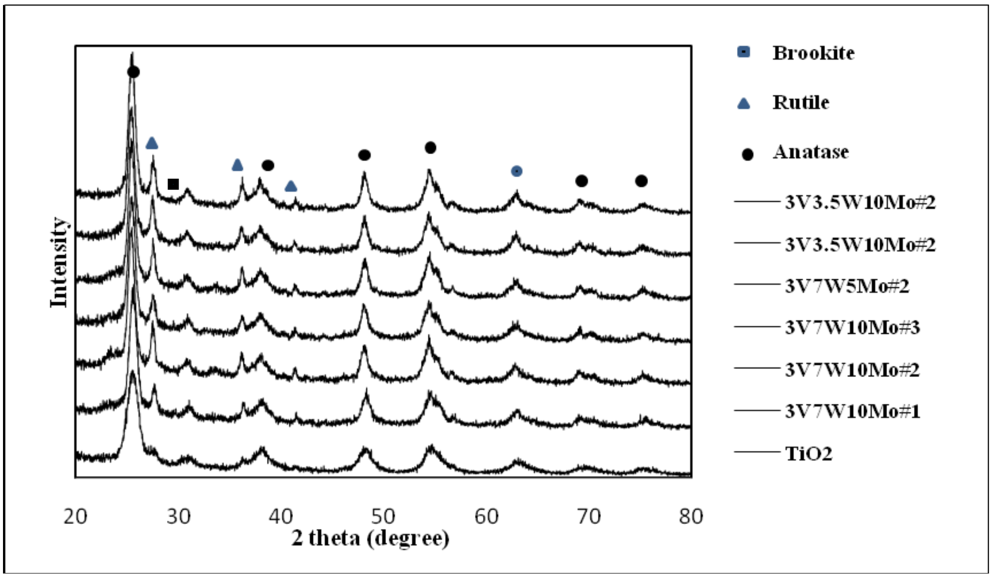

Figure 3.13 XRD patterns of V_2O_5-WO_3-MoO_3/TiO_2 catalysts.

3.2.5 Fourier Transforms Infrared (FT-IR)

The functional group on the catalyst surface was determined by FT-IR using Nicolet model Impact 6700 of the IR spectrometer. Infrared spectra are recorded between 400 and 4000 cm^{-1} on a microcomputer.

The functional groups of the V_2O_5-WO_3-MoO_3/TiO_2 catalysts were determined by this technique. Figures 3.14-3.19 show FT-IR spectra of all catalysts. Three peaks of the all spectra that were absorbed are reported in the (400-1200) cm^{-1} range. The results show two strong absorption at 707 cm^{-1}, the typical of TiO_2 anatase and 764 cm^{-1}, the W=O stretching of wolframyl species. The weak band on the shoulder near 974 cm^{-1} is assigned to the composite oxide of vanadium and molybdenum. In addition no peak of V_2O_5 and MoO_3 passed absorption band.

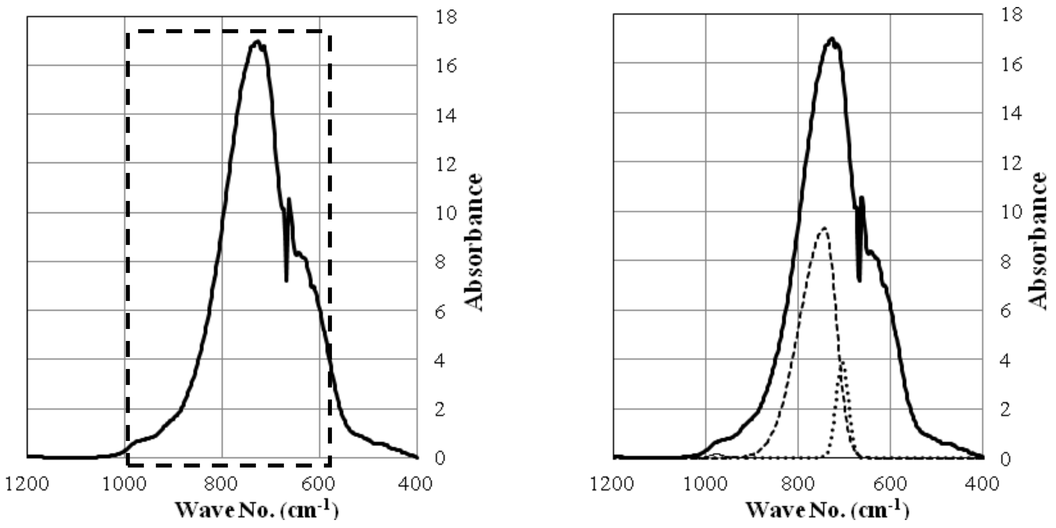

Figure 3.14 FT-IR spectrum of 3V7W10Mo#1 catalyst. (Warinsiriux, 2011)

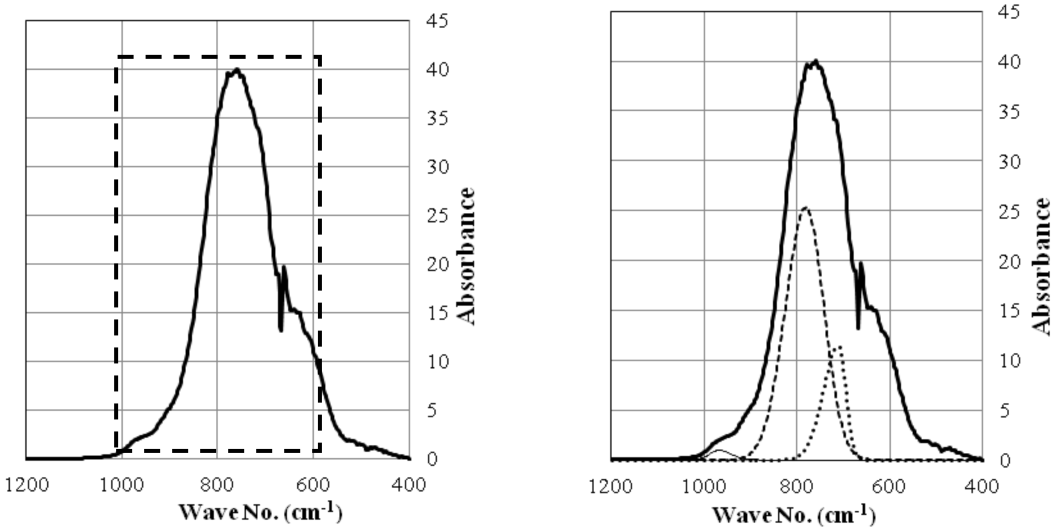

Figure 3.15 FT-IR spectrum of 3V7W10Mo #2 catalyst. (Warinsiriux, 2011)

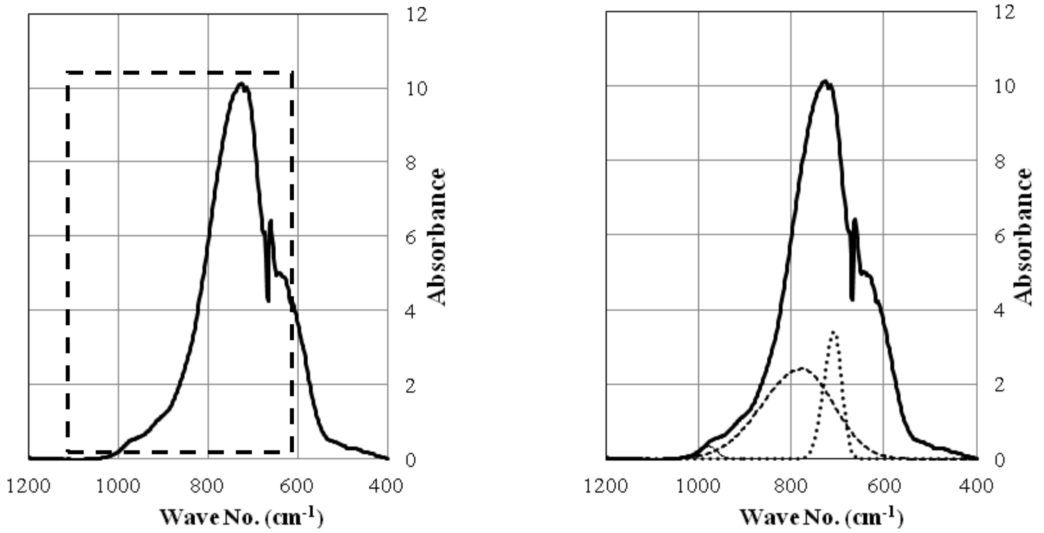

Figure 3.16 FT-IR spectrum of 3V7W10Mo#3 catalyst. (Warinsiriux, 2011)

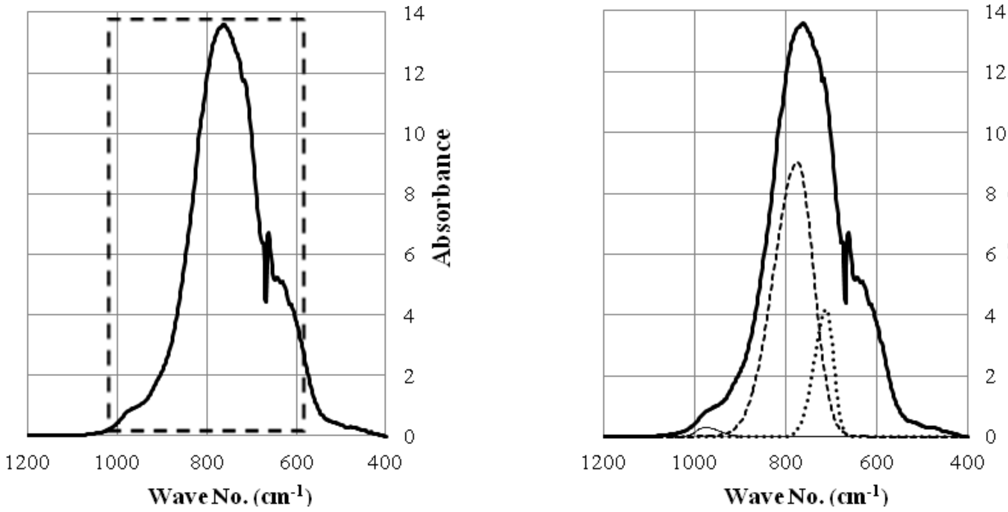

Figure 3.17 FT-IR spectrum of 3V7W5Mo#2 catalyst. (Warinsiriux, 2011)

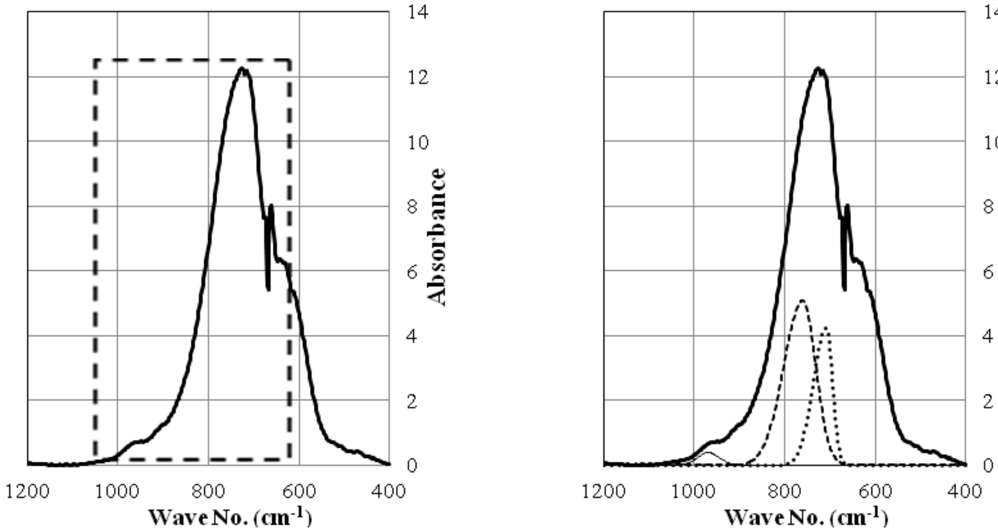

Figure 3.18 FT-IR spectrum of 3V3.5W10Mo#2 catalyst. (Warinsiriux, 2011)

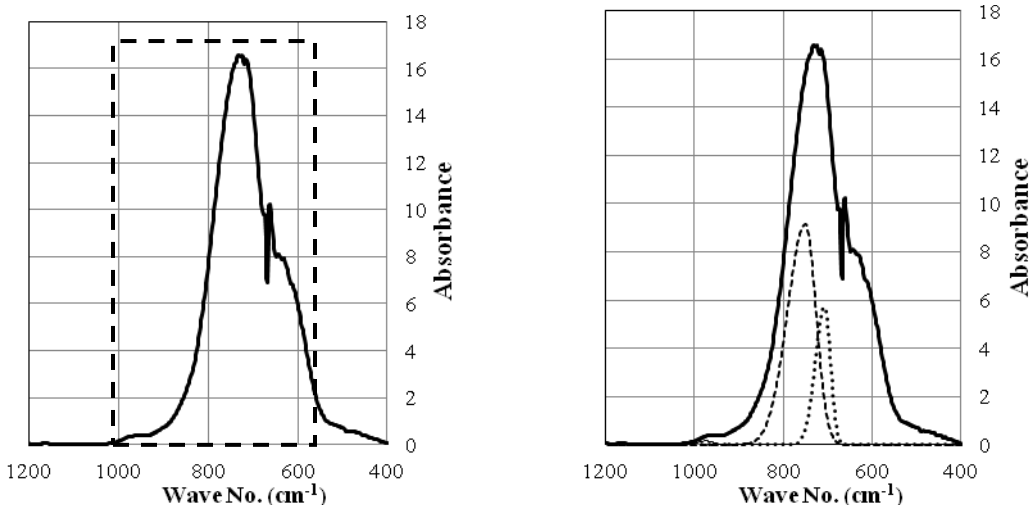

Figure 3.19 FT-IR spectrum of 3V3.5W5Mo#2 catalyst. (Warinsiriux, 2011)

3.3 Catalytic activity testing

All prepared catalysts are tested on selective catalytic reduction of NO_x with ammonia, NH_3 oxidation and SO_2 oxidation to determine the formation N_2O and SO_3 that occurs in the SCR process. The flue gas simulates that of a real power plant with various gases, such as nitric oxide (NO), oxygen (O_2), sulfur dioxide (SO_2), and water (H_2O) as shown in table 3.5

Table 3.5 The concentration of flue gases that simulates that of a real power plant.

Feed gases	Concentration
NO	120 ppm
O_2	15% vol
SO_2	30 ppm
H_2O	15%vol
N_2	balanced

3.3.1 Selective catalytic reduction of NO_x with NH_3 testing

The selective catalytic reduction of NO_x with NH_3 is one of the methods for catalytic activity testing to determine removal NO_x and formation of N_2O. The feed gas composes of NO, NH_3, O_2, H_2O, SO_2 and N_2. The concentration of the feed gas and volumetric flow rate of each gas were adjusted by mass flow controller. Total volumetric flow rate is approximately 230 ml/min and WHSV 120,000 ml/g.min as shows in table 3.6. The feed gases flow through a stainless tubular fixed bed reactor with a outside diameter of 3/8 in (SS-314) which contains a catalyst packing of 0.1 g on quartz wool. Operating condition varies between 120°C and 450°C. An electric furnace was supplied heat to a reactor. The temperatures in the furnaces were control by a digital temperature controller. (see figure 3.20)

Shimadzu GC-2014 equipped with an Electron Capture Detector (ECD) measures the concentration of NO_x and N_2O in the outlet stream. Detail of operating condition of the GC-2014 to analyze NO and N_2O show in table 3.7.

Table 3.6 The composition and concentration of feed gases for SCR process.

Feed gases	Concentration
NO	120 ppm
NH_3	120 ppm
O_2	15% vol
SO_2	30 ppm
H_2O	15%vol
N_2	balanced

Table 3.7 The operating condition of Shimadzu GC-2014 for analyzing in the SCR process.

Shimadzu GC-2014	**Analyzed gas**		
	NO	**N_2O**	**SO_2**
Detector	ECD	ECD	FPD
Temp Detector (°C)	200	200	185
Column	Hyasep-DB	Hyasep-DB	Rt-XL sulfur
Max temperature column (°C)	190	190	240
Temperature column (°C)	40	150	180
Inner Diameter column (mm)	0.1	0.1	1
Length column (m)	2	2	2
Temperature injector (°C)	-	-	100
Carrier gas	N_2	N_2	He
Carrier gas flow	240 kPa	240 kPa	15ml/min
Add flow (kPa)	-	-	Air:35 H_2:105
Sampling rate (msec)	80	80	40

ECD: Electron Capture Detector **FPD: Frame Photometric Detector**

3.3.2 Ammonia oxidation testing

The ammonia oxidation is main side reaction of SCR process bring about the NO_x reduction conversion decrease at high temperature, therefore measuring NO_x that is appear during SCR process is necessary. The feed gas composes of NH_3, O_2 and N_2. The concentration of the gases and volumetric flow rate of each gas were adjusted by mass flow controller. Total volumetric flow rate is approximately 230 ml/min and WSHV 138,000 ml/g.min as shows in table 3.8. The feed gases flow through a stainless tubular fixed bed reactor with a outside diameter of 3/8 in (SS-314) which contains a catalyst packing of 0.1 g on quartz wool. Operating condition varies between 120°C and 450°C. An electric furnace was supplied heat to a reactor. The temperatures in the furnaces were control by a digital temperature controller.

Table 3.8 The composition and concentration of feed gases for ammonia oxidation process.

Feed gases	**Concentration**
NH_3	120 ppm
O_2	15% vol
N_2	balanced

The concentration of NO_x was measured by Shimadzu GC-2014 equipped with an Electron Capture Detector (ECD). The operating condition for GC-2014 is same the SCR process as show in table 3.7.

3.3.3 Sulfur dioxide oxidation

Sulfur dioxide can be oxidized to sulfur trioxide catalytically. The common catalyst is vanadium (V) oxide (V_2O_5). Because the prepared SCR catalyst is V_2O_5-WO_3-MoO_3/TiO_2 as possible occurring SO_2 oxidation and generates sulfur trioxide that can produce ammonium bisulfate result from reacts with unconverted NH_3 bring about a sticky, corrosive compound, which fouls heat exchangers and other equipment downstream thus it is necessary to measure SO_2.

The feed gas composes of SO_2, NO, O_2 and N_2. The concentration of the gases and volumetric flow rate of each gas were adjusted by mass flow controller. Total volumetric flow rate is approximately 230 ml/min and WSHV 138,000 ml/g.min as shows in table 3.9. The feed gases flow through a stainless tubular fixed bed reactor with an outside diameter of 3/8 in (SS-314) which contains a catalyst packing of 0.1 g on quartz wool. Operating condition varies between 120°C and 450°C. An electric furnace was supplied heat to a reactor. The temperatures in the furnaces were control by a digital temperature controller.

Table 3.9 The composition and concentration of feed gases for sulfur dioxide oxidation process.

Feed gases	**Concentration**
SO_2	30 ppm
O_2	15%vol
NO	120 ppm
N_2	balanced

The concentration of SO_2 was measured by Shimadzu GC-2014 equipped with a Flame Photometric Detector (FPD). The operating condition for measuring SO_2 concentration is show in table 3.7.

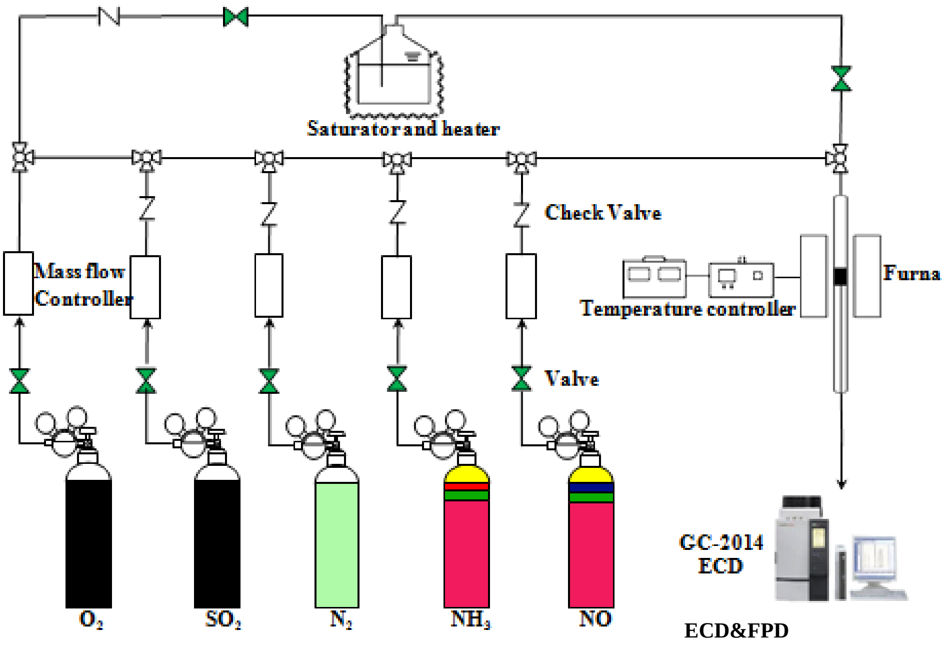

Figure 3.20 Flow diagram of the reactor system for SCR of NO by NH_3, NH_3 oxidation and SO_2 oxidation.

CHAPTER IV

RESULTS AND DISCUSSION

This chapter shows results and discussion of the catalytic activities testing. The chapter is divided in to three major sections. The first section (4.1) summarizes the experimental results obtained from the oxidation of SO_2 to SO_3 over all V_2O_5-WO_3-MoO_3/TiO_2 catalysts studied in this research.

The second section (4.2) reports the selective catalytic reduction performance, the formation of N_2O, and the oxidation of NH_3 to NO over all V_2O_5-WO_3-MoO_3/TiO_2 catalysts studied in the present work. This section is further divided in to two sub-sections. The first sub-section (4.2.1) compares the behavior of catalysts having the same composition, but prepared from different procedures (3V7W10Mo#1, 3V7W10Mo#2 and 3V7W10Mo#3). The second sub-section (4.2.2) compares the behavior of catalysts having different compositions (3V7W5Mo#2, 3V3.5W10Mo#2 and 3V3.5W5Mo#2).

The last section (4.3) is the discussion on the reaction path ways occurring during the selective catalytic reduction of NO with NH_3.

4.1. Formation of SO_3 over V_2O_5-WO_3-MoO_3/TiO_2 catalysts.

In the SO_2 oxidation experiments, water was removed from the feed stream in order to avoid dissolution of SO_3 (if occurs) in condensed water vapor which may present in some part of tubing system where heating is not sufficient.

The concentration of SO_2 measured at the outlet of reactor of all catalysts and TiO_2 support are reported in figure 4.1 and table 4.1. From the figure one can see that the outlet concentration of SO_2 begins to decrease from the reaction temperatures 250°C. This decrease is also observed even though TiO_2 is used. In addition, no peak of SO_3 appears on any chromatograms. These two phenomena (decrease of SO_2 when TiO_2 is used and disappearance of SO_3 peak) suggest that the reaction of SO_2 concentration at the outlet at high temperatures is not the result of the oxidation of

SO_2 to SO_3. The real cause is the effect of the back pressure, at the outlet of the SO_2 mass flow controller, with increase when the reactor temperatures increase.

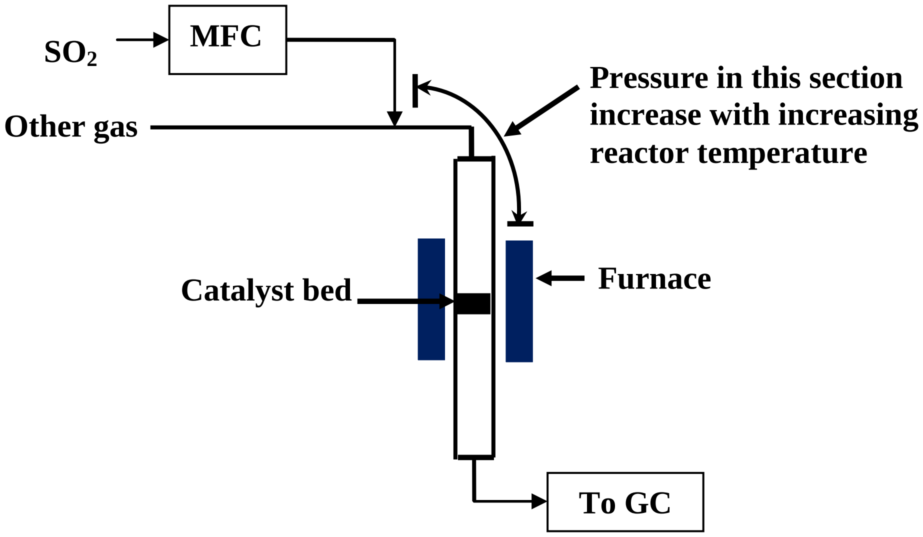

Figure 4.1 A simplified diagram of the reactor system.

Since the concentration of SO_2 used in our experiments is very low. The valve opening of the SO_2 mass flow controller is therefore very low (0.45 from 10 full scale or equivalent to 0.6 ml/min at the supply pressure 2 barg). When the back pressure increases, the differential pressure across the valve decreases. This phenomena reduces the actual flow rate of SO_2. This explanation is confirms by performing experiment by packing TiO_2 support having different pack density into the reactor. The higher pack density results in the higher back pressure. It is observed that at too high packing decreasingly the SO_2 mass flow controller will lose the capability to control the flow rate of SO_2 gas.

Therefore we can conclude that all the catalysts used in this research under the operating condition studies have insignificant SO_2 oxidation to SO_3 capability.

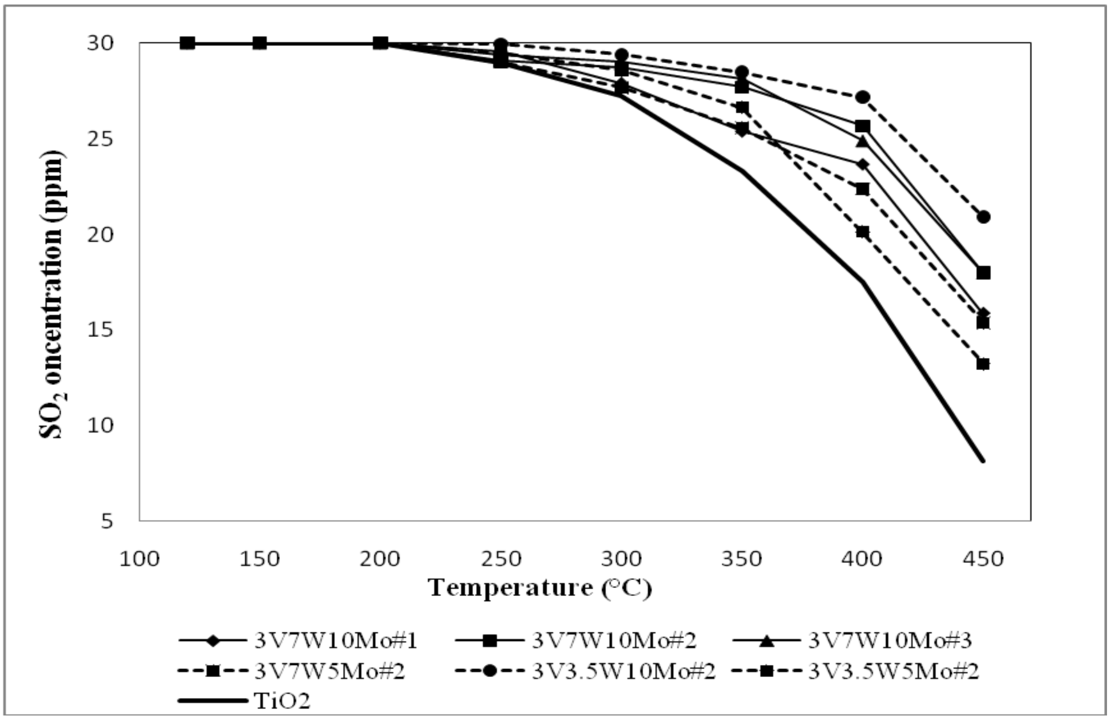

Figure 4.2 Outlet concentration of SO_2 of V_2O_5-WO_3-MoO_3/TiO_2 catalysts and TiO_2-support at various temperatures. Reaction condition: [SO_2] = 30 ppm, [O_2] = 15%vol, [NO]= 30 ppm, N_2 balanced for WSHV =120,000 ml/g.h.

Table 4.1 Data for figure 4.2 (concentration of SO_2-ppm)

Sample	**Temperature (°C)**							
	120	**150**	**200**	**250**	**300**	**350**	**400**	**450**
3V7W10Mo#1	30	30	30	29.56	27.89	25.38	23.66	15.87
3V7W10Mo#2	30	30	30	29.09	28.71	27.69	25.67	18.01
3V7W10Mo#3	30	30	30	29.41	29.04	28.16	24.89	17.98
3V7W5Mo#2	30	30	30	29.01	27.66	25.56	22.36	15.38
3V3.5W10Mo#2	30	30	30	29.94	29.39	28.48	27.17	20.90
3V3.5W5Mo#2	30	30	30	29.47	28.56	26.63	20.14	13.22
TiO_2	30	30	30	29.01	27.25	23.30	17.54	8.14

4.2. The selective catalytic reduction performance over V_2O_5-WO_3-MoO_3/TiO_2 catalysts.

This section is further divided in to two sub-sections. The first sub-section (4.2.1) compares the behavior of catalysts having the same composition, but prepared from different procedures (3V7W10Mo#1, 3V7W10Mo#2 and 3V7W10Mo#3).The second sub-section (4.2.2) compares the behavior of catalysts having different compositions (3V7W5Mo#2, 3V3.5W10Mo#2 and 3V3.5W5Mo#2).

4.2.1 Behavior of catalysts having the same composition and different procedure.

The catalysts reported in this section have the same composition, but prepared from different procedures (3V7W10Mo#1, 3V7W10Mo#2 and 3V7W10Mo#3) as described previously in section 3.1. The catalysts were tested by the selective catalytic reduction of NO with NH_3 and NH_3 oxidation as described in sections 3.3.1-3.3.2. The results are showed in figures 4.3-4.5.

3V7W10Mo#1 catalyst begins to exhibits NO conversion at reaction temperature 120°C. The NO conversion increases up to level higher than 80% at the reaction temperature around 200°C and remains at this level up to 300°C before rapidly drop. The formation of N_2O appears when the decrease of NO conversion appears. In addition, the oxidation NH_3 to NO carried out in a separate experiment show that NH_3 can be oxidize by O_2 to NO at the same temperatures.

3V7W10Mo#2 catalyst exhibits higher NO conversion at 120°C, than as 3V7W10Mo#1 (32% versus 2%). The NO conversion increases up to level higher than 80% at the reaction temperature around 200°C and remains at this level up to 350°C before rapidly drop. The formation of N_2O appears before the decrease of NO conversion become pronounce. In addition, the oxidation NH_3 to NO carried out in a separate experiment show that NH_3 can be oxidize by O_2 to NO at the same temperatures that N_2O appears.

The NO conversion curve of 3V7W10Mo#3 catalyst has the same pattern as of 3V7W10Mo#1 and 3V7W10Mo#2. This catalyst achieves only 60% NO conversion at 200°C. And interesting phenomenon observed is the formation of N_2O is observed at the temperature lower than the oxidation of NH_3 begins.

Since the catalyst prepared by using the second procedure (3V7W10Mo#2) has high NO conversion and widest operating temperatures. Because of these reasons the catalysts prepared by using second procedure, but having different Mo and W loading (3V7W5Mo#2, 3V3.5W10Mo#2 and 3V3.5W5Mo#2) are further investigated. The results are reported in section 4.2.2.

The discussion on the main reactions involve during the selective catalytic reduction of NO with NH_3 process will be discus in section 4.3

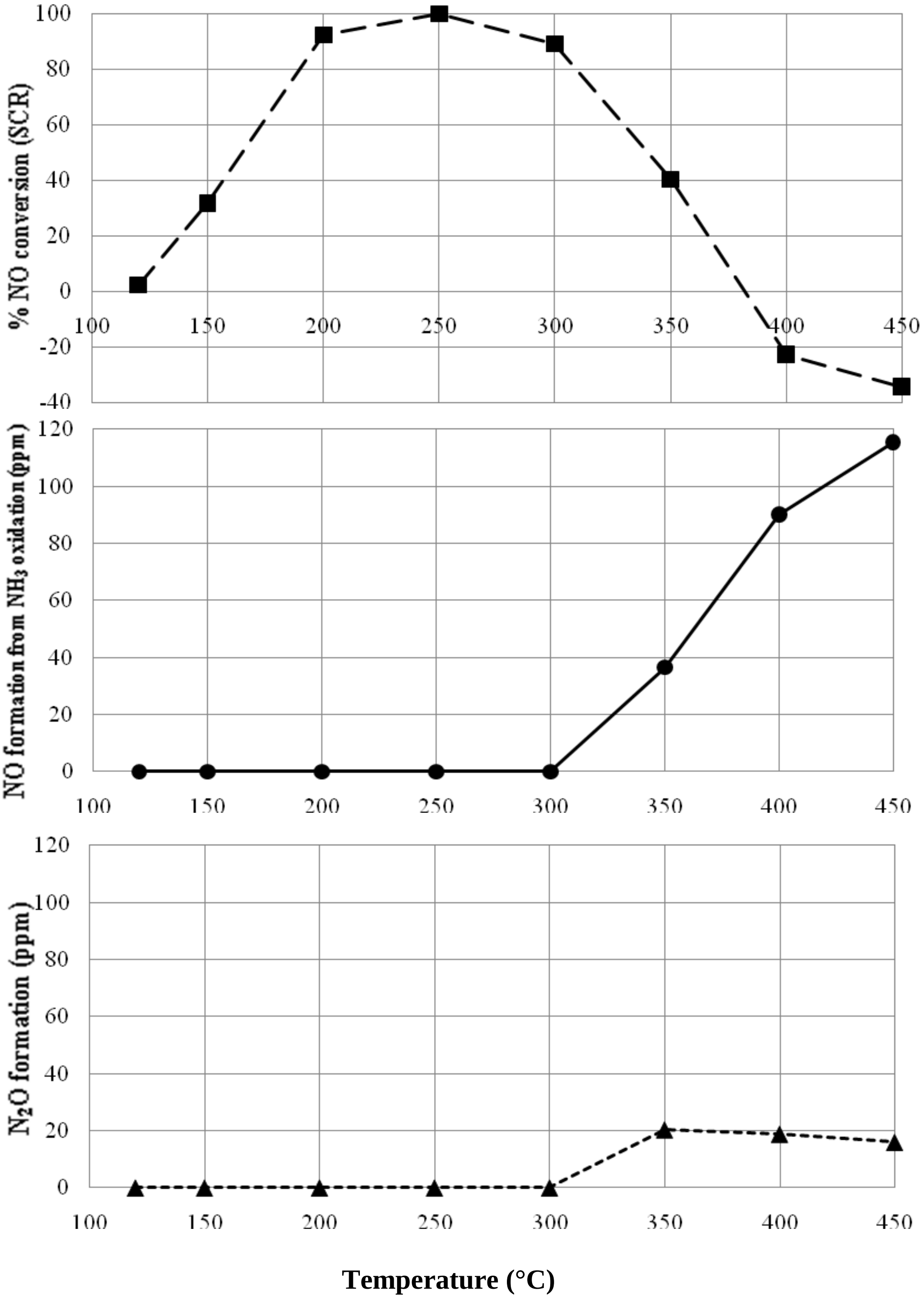

Figure 4.3 Catalytic activities testing on 3V7W10Mo#1 catalyst at 120°C-450°C.

Table 4.2 Data for figure 4.3.

Temperature (°C)	**NO reduction conversion (%)**	**[NO] from NH_3 oxidation (ppm)**	**[N_2O] from SCR (ppm)**
120	2.39	0	0
150	31.82	0	0
200	92.48	0	0
250	100	0	0
300	89.19	0	0
350	40.46	36.50	20.34
400	-22.66	90.17	18.78
450	-34.31	115.59	15.95

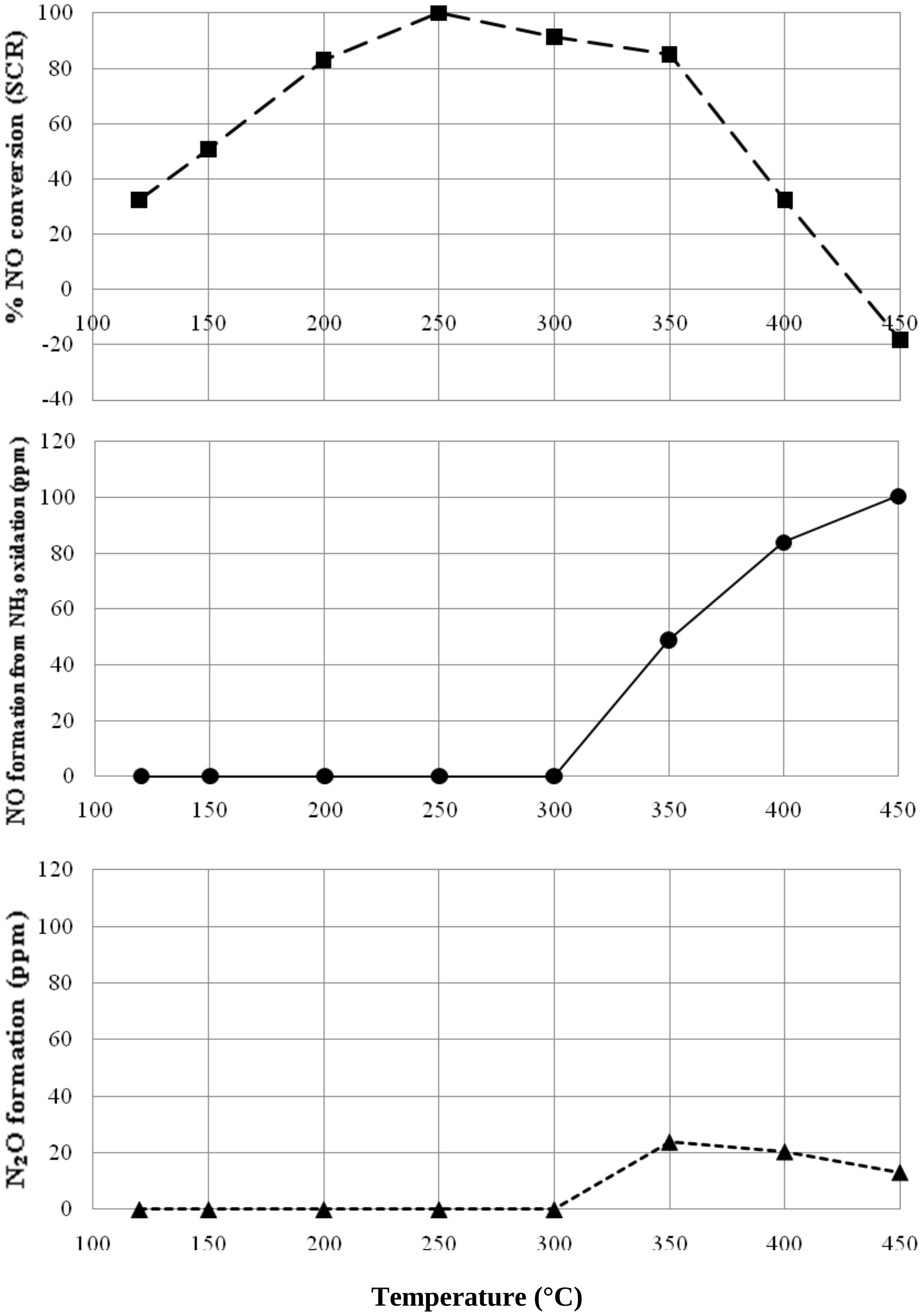

Figure 4.4 Catalytic activities testing on 3V7W10Mo#2 catalyst at 120°C-450°C.

Table 4.3 Data for figure 4.4.

Temperature (°C)	**NO reduction conversion (%)**	**[NO] from NH_3 oxidation (ppm)**	**[N_2O] from SCR (ppm)**
120	32.37	0	0
150	50.81	0	0
200	82.96	0	0
250	100	0	0
300	91.45	0	0
350	84.99	48.84	23.79
400	32.42	83.90	20.40
450	-18.25	100.45	13.12

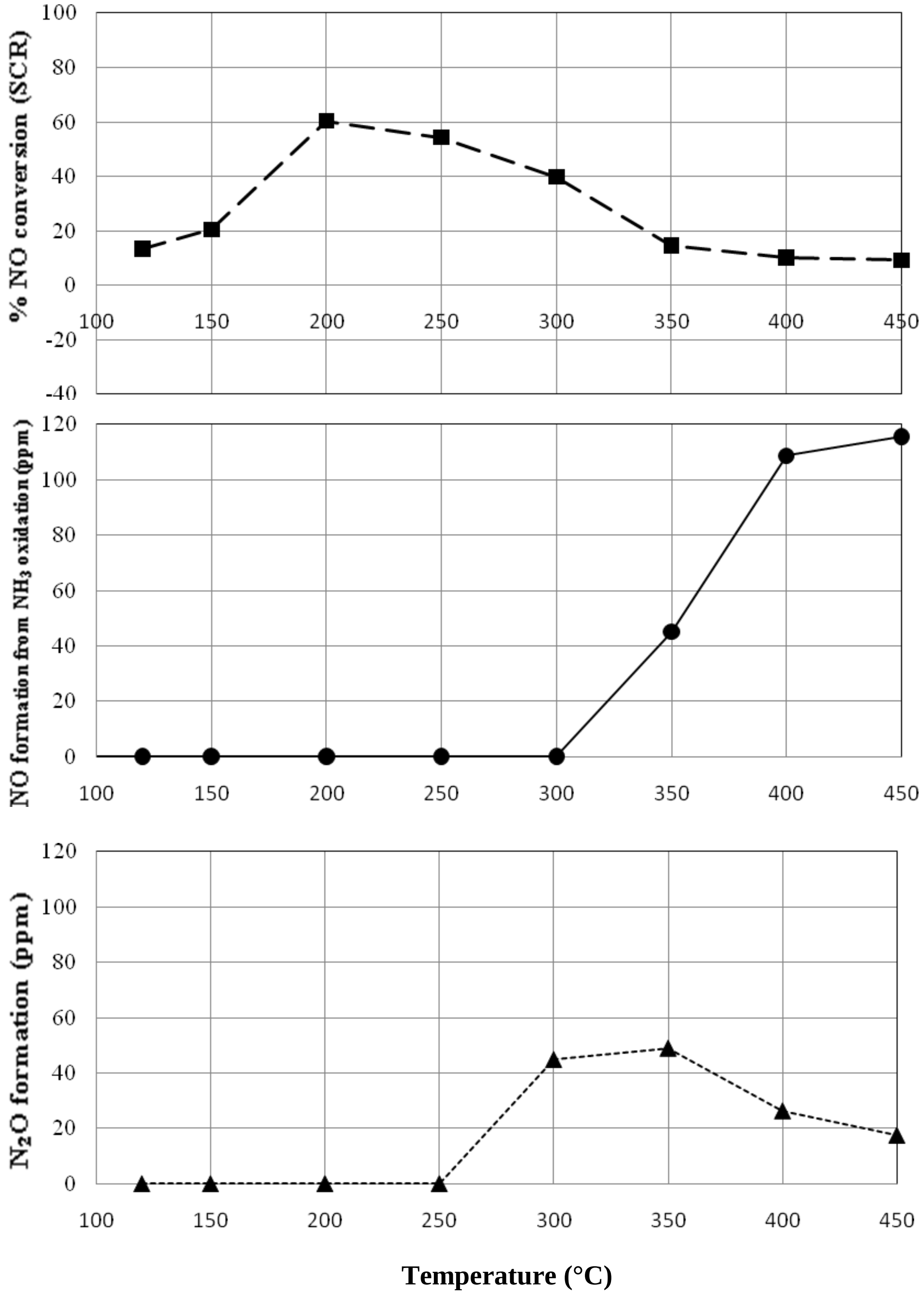

Figure 4.5 Catalytic activities testing on 3V7W10Mo#3 catalyst at 120°C-450°C

Table 4.4 Data for figure 4.5.

Temperature (°C)	**NO reduction conversion (%)**	**[NO] from NH_3 oxidation (ppm)**	**[N_2O] from SCR (ppm)**
120	13.31	0	0
150	20.52	0	0
200	60.37	0	0
250	54.33	0	0
300	39.83	0	44.80
350	14.62	45.11	48.85
400	10.20	108.70	26.25
450	9.24	115.57	17.47

4.2.2 Behavior of catalysts having the same procedure preparation and different composition.

The catalysts reported in this section have the same preparation procedure, but having different compositions (3V7W5Mo#2, 3V3.5W10Mo#2 and 3V3.5W5Mo#2) as described in section 3.1. The catalysts were tested by the selective catalytic reduction of NO with NH_3 and NH_3 oxidation as described in sections 3.3.1-3.3.2. The results are showed in figures 4.6-4.8.

3V7W5Mo#2 catalyst exhibits significantly high NO conversion at reaction temperature 120°C. The NO conversion increases up to level higher than 80% at the reaction temperature around 200°C and remains at this level up to 250°C before slightly decrease at 300°C and rapidly drop at 350°C. The formation of N_2O appears when the decrease of NO conversion appears. In addition, the oxidation NH_3 to NO carried out in a separate experiment show that NH_3 can be oxidize by O_2 to NO at the same temperatures.

3V3.5W10Mo#2 catalyst also begins to exhibit NO conversion at 120°C, the same as 3V7W5Mo#2, but with lower conversion (3% versus 32%). The NO conversion increases up to about 60% at the reaction temperature around 250°C before rapidly drop. The formation of N_2O appears before the decrease of NO conversion become pronounce. In addition, the oxidation NH_3 to NO carried out in a separate experiment show that NH_3 can be oxidize by O_2 to NO at the same temperatures that N_2O appears.

The NO conversion curve of 3V3.5W5Mo#2 catalyst as the same pattern of 3V7W5Mo#2 and 3V3.5W10Mo#2. This catalyst achieves only 70% NO conversion at 200°C and interesting phenomenon is the formation of N_2O is observed at the temperature lower than the oxidation of NH_3 begins.

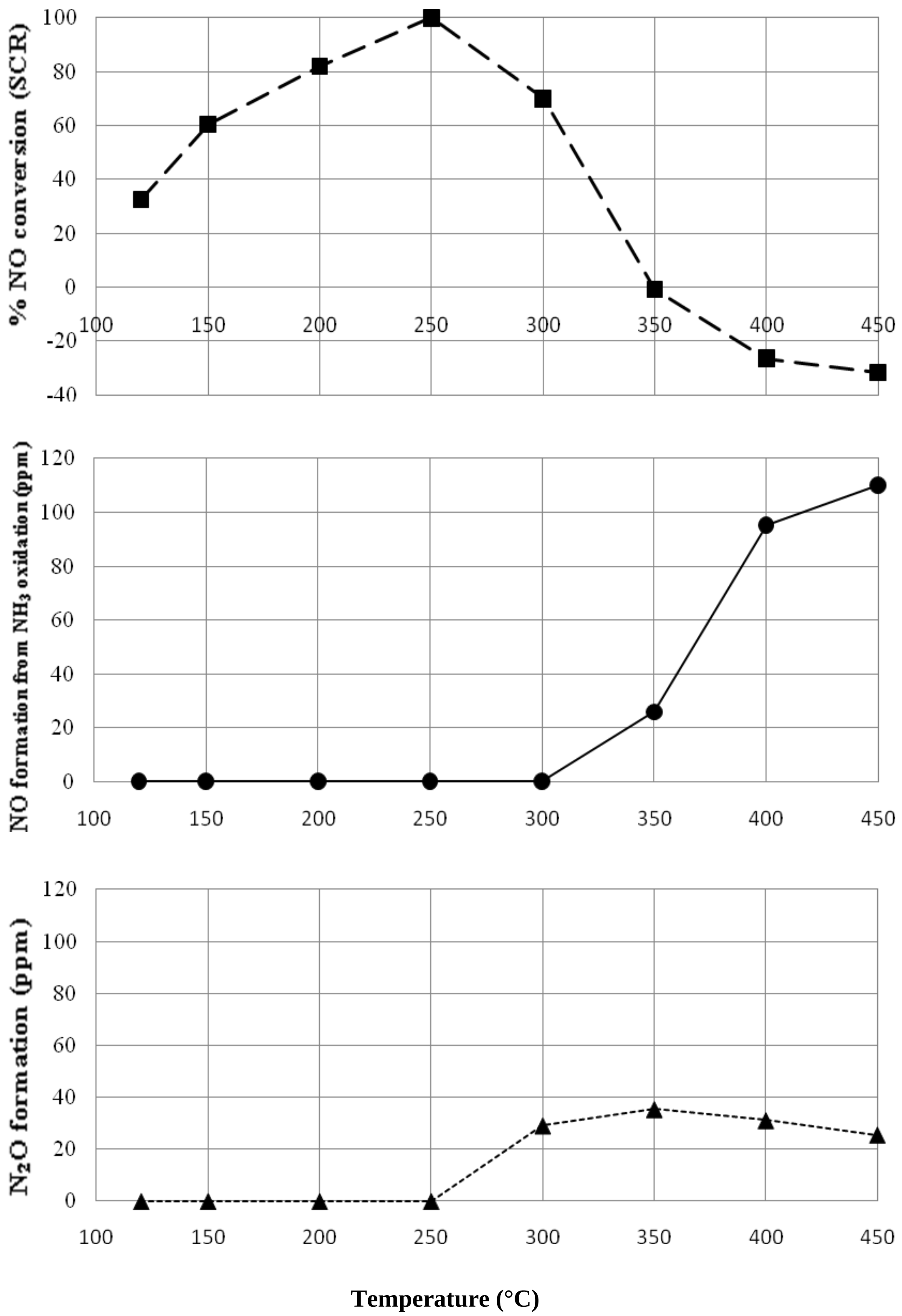

Figure 4.6 Catalytic activities testing on 3V7W5Mo#2 catalyst at 120°C-450°C.

Table 4.5 Data for figure 4.6.

Temperature (°C)	**NO reduction conversion (%)**	**[NO] from NH_3 oxidation (ppm)**	**[N_2O] from SCR (ppm)**
120	32.48	0	0
150	60.43	0	0
200	82	0	0
250	100	0	0
300	70	0	29.20
350	-0.77	25.87	35.46
400	-26.52	95.17	31.21
450	-31.73	110.08	25.61

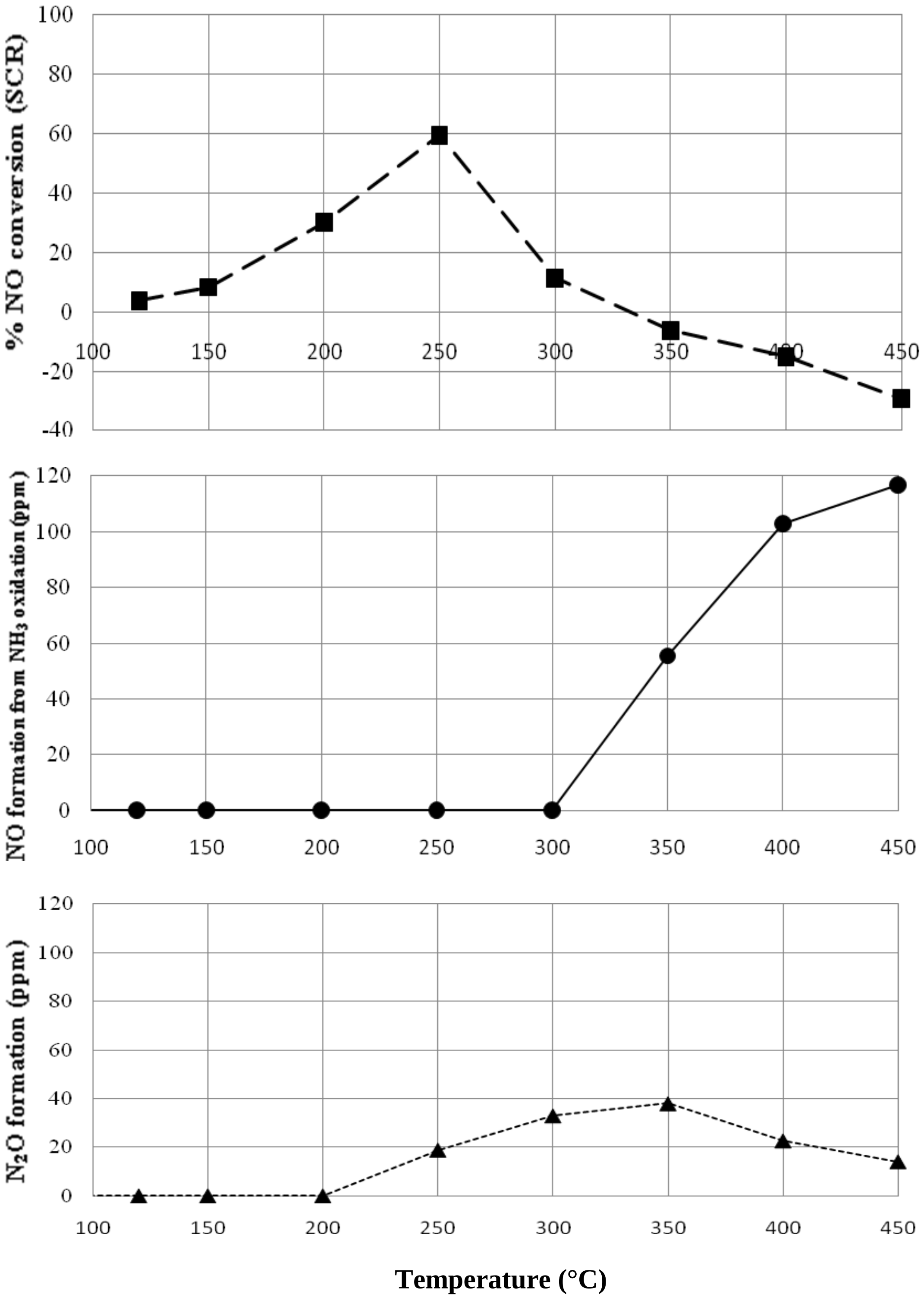

Figure 4.7 Catalytic activities testing on 3V3.5W10Mo#2 catalyst at 120°C-450°C.

Table 4.6 Data for figure 4.7.

Temperature (°C)	NO reduction conversion (%)	[NO] from NH_3 oxidation (ppm)	[N_2O] from SCR (ppm)
120	3.79	0	0
150	8.39	0	0
200	30.18	0	0
250	59.56	0	18.88
300	11.43	0	33.05
350	-6.31	55.42	38.06
400	-15.09	102.95	22.70
450	-29.26	116.86	14.10

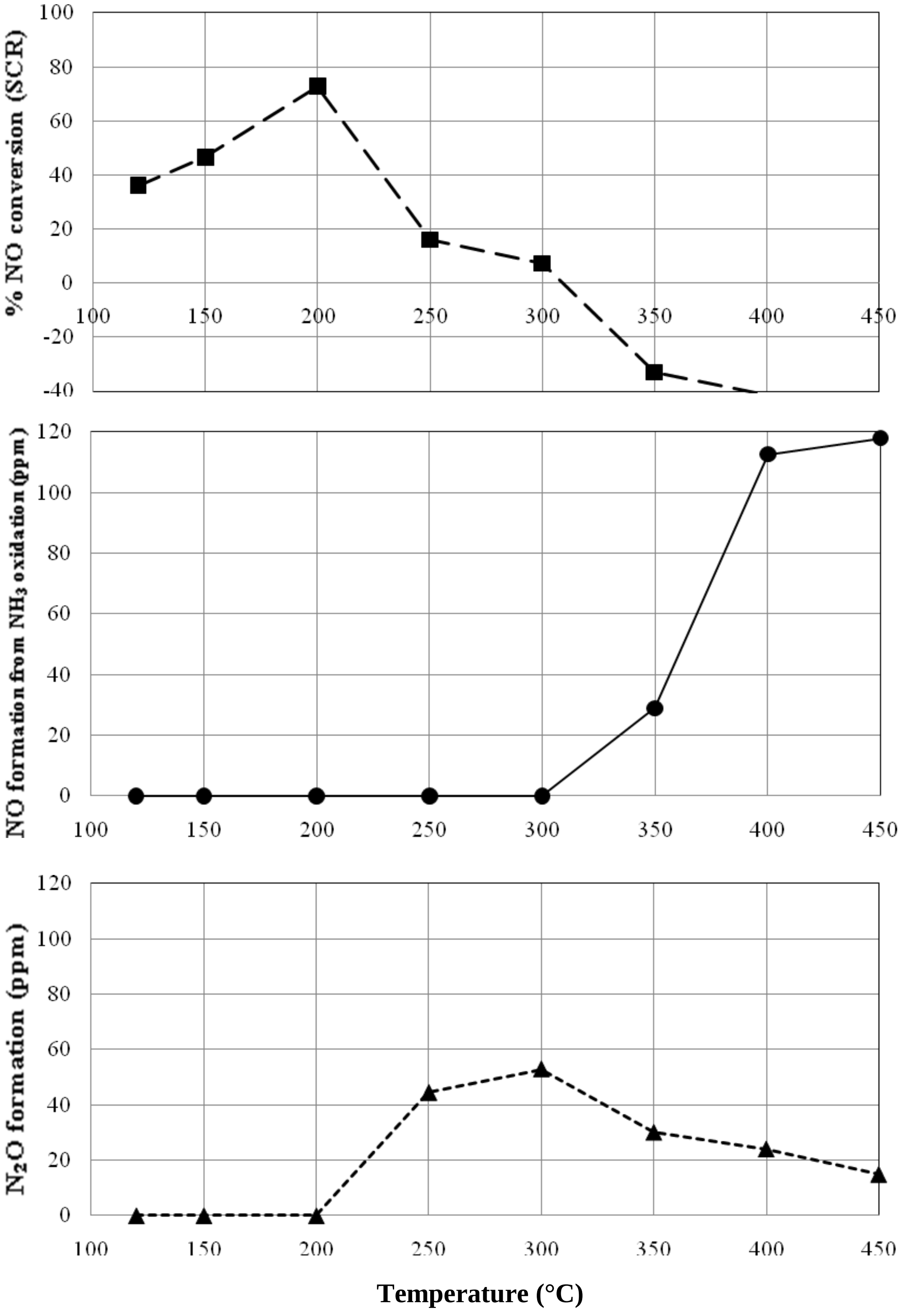

Figure 4.8 Catalytic activities testing on 3V3.5W5Mo#2 catalyst at 120°C-450°C.

Table 4.7 Data for figure 4.8.

Temperature (°C)	**NO reduction conversion (%)**	**[NO] from NH_3 oxidation (ppm)**	**[N_2O] from SCR (ppm)**
120	36.08	0	0
150	46.63	0	0
200	72.79	0	0
250	16.04	0	44.41
300	7.30	0	52.91
350	-33.01	28.93	30.08
400	-41.30	112.67	24.06
450	-43.69	118.00	14.92

4.3 The reaction path way occurring during the selective catalytic reduction of NO with NH_3.

Three possible mechanism which can described the selective catalytic reduction of NO_x with NH_3 are Eley-Rideal, Reduction-Oxidation (ReDox) mechanism and homogeneous reaction mechanism.

1. Eley-Rideal mechanism is proposed in 1938 by D. D.Eley and E. K.Rideal. In this mechanism only one of the molecules adsorbs and the other one reacts with it directly from the gas phase, without adsorbing. This mechanism is showed below.

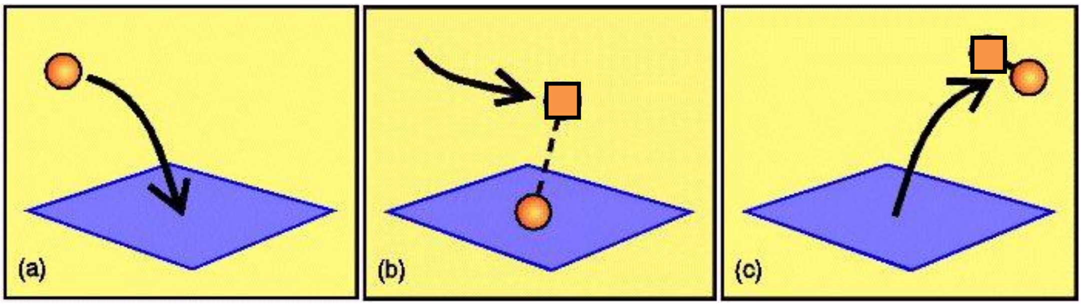

(a) An atom adsorbs on the surface
(b) Another atom passes by which interacts with the one on the surface.
(c) A molecule is formed which desorbed

Figure 4.9 Eley-Rideal Mechanism

2. Reduction-Oxidation (REDOX) mechanism proposed in 1954 by Mars and van Krevelenv (Mar and van Krevelenv, 1954), the molecule is adsorbed on the catalyst surface, using an oxygen vacancy in the lattice of the oxide as a deposition place for one of its oxygen atom. This mechanism can be written follow:

$$A + \text{(oxidized catalyst)} \rightarrow P + \text{(reduced catalyst)} \qquad \text{(eq. 4.1)}$$

$$O_2 + \text{(reduced catalyst)} \rightarrow \text{(oxidized catalyst)} \qquad \text{(eq. 4.2)}$$

3. Homogeneous Reaction mechanism, the reaction is chemical reactions in which the reactants are in the same phase.

During the SCR process the followings reactions are hypothesized

I. Adsorption of NH_3 on catalyst surface, NO form gases phase reacts with NH_3.

II. Adsorption of NH_3 on catalyst surface, O_2 form gases phase reacts with NH_3.

These hypothesizes (I and II) are followed by Eley-Rideal mechanism. This mechanism is limited by the ability of catalyst surface to hold NH_3 molecules on its surface. The ability of the catalyst to hold the NH_3 can be quantified from NH_3-TPD result. This mechanism is not likely to occurs at low temperature.

III. NH_3 molecule reacts with lattice oxygen at the catalyst surface result in the reduction of the catalyst surface. Then NO molecule oxidized the catalyst surface back to the normal state.

IV. NH_3 molecule reacts with lattice oxygen at the catalyst surface result in the reduction of the catalyst surface. Then O_2 molecule oxidized the catalyst surface back to the normal state.

These hypothesize are follows by REDOX mechanism. This mechanism is not likely to occur at high temperature.

V. Homogeneous reaction, gas phase NH_3 react with NO

VI. Homogeneous reaction, gas phase NH_3 react with O_2

These reactions (V-VI) are not dependent on the catalyst, but depend on the temperature.

4.3.1 The selective catalytic reduction in the low reaction temperature region

The selective catalytic reduction at low reaction temperature region here mean from the 120°C to the maximum conversion NO. The mechanism in this low reaction temperature region was proposed by Langmier-Hinsherwood, but in our opinion Eley-Rideal is more reasonable because of the following reason:

1) Normally, the surface of metal oxide composes of cation and anion species. These species prefer adsorb polar molecules such as ammonia in our case.

2) The adsorption of non-polar molecule such as O_2 and NO on metal oxide surface can occur if the oxide surface is oxidized or reduced (Bond, 1987). For instant when transition metal (V, W, Mo) are in there highest oxidation state, the adsorption of the non-polar molecules (O_2, NO) can occur when these oxides reduced to a lower oxidation state. The meaning of reduction here is the loss of O^{-2} to O_2 without the involvement of any reducing agents (such as NH_3, H_2, CO). This reduction process normally requires high temperature in order of several hundred degree celsius.

Therefore the mechanism at low temperature should be following the the reason 1 and 2. If we look at the NO conversion curve and NH_3 oxidation curve, we can see that the oxidation of NH_3 by O_2 (in the absence NO) at reaction temperature higher than the reaction of NO conversion. (see in figures 4.3-4.8), thus the selective catalytic reduction of NO with NH_3 at low temperature followed by Eley-Rideal mechanism and according to hypothesis I.

4.3.2 The selective catalytic reduction at high reaction temperature region

At high reaction temperature the amount of adsorbed NH_3 on the catalyst surface is lower than at low reaction temperature. (see figures 3.4-3.10: NH_3-TPD profiles) This phenomenon leads to lower reaction rate. On the contrary the rate constant increases result in reaction rate increases. The overall reaction rate depend on with factor plays the dominate role.

4.3.3 Formation of N_2O during the selective catalytic reduction

For the catalysts having the same compositions, but different method of preparation we found that difference in SCR activity is observed. All three catalysts (3V7W10Mo#1, 3V7W10Mo#2 and 3V7W10Mo#3) have similar NH_3 oxidation result. However, the catalyst having the lowest NO conversion, having the highest N_2O formation.

The question we are fa now is “Where N_2O come from”

a) Reaction between NH_3 and NO and/or

b) Reaction between NH_3 and O_2

At high temperature, the decrease of selective catalytic reduction activity is the result of

c) The desorption of NH_3 on catalyst surface and/or

d) The loss of NH_3 via the NH_3 oxidation by O_2 to NO

In order to specify the source of N_2O, the data of 3V7W10Mo#2 was used because this catalyst produce N_2O while the NO conversion still very high at 350°C this catalyst has 85% NO conversion with mean that 102 ppm of NH_3 must be consume in the reaction with NO. At this temperature N_2O produce 20 ppm and NH_3

oxidation, NH_3 loss by the oxidation with O_2 (in the absence of NO) can be as high 50 ppm.

If N_2O is produce from the reaction between NH_3 and O_2 there will be no enough NH_3 for the SCR process to achieve 85% NO conversion therefore should come from the reaction between NO and NH_3.

Another interesting point is tungsten play an important role in the selective catalytic reduction reaction, N_2O formation in the high reaction temperature region reduction in tungsten loading cause via reduction in NO conversion (3V7W10Mo#2 and 3V3.5W10Mo#2 in figures 4.4 and 4.6), but N_2O formation increase significantly. Decrease the amount of Mo content less pronounces effect on the decrease in the SCR conversion and N_2O formation (see result of 3V7W10Mo#2 and 3V7W5Mo#2 in figures 4.4-4.5).

4.3.4 Oxidation of NH_3

It was consider the highest temperature NH_3 can be adsorbed on the catalyst surface (further NH_3-TPD results reported in section 3.3.2), we can see that at the temperature NH_3 began to be oxidized, less small amount or none of NH_3 can be adsorbed on the catalyst surface. Therefore, the oxidation of NH_3 to NO should not proceed via the same mechanism as the SCR (Eley-Rideal mechanism). Homogeneous reaction between NH_3 and O_2 is known to be able to occur at high temperature. But the amount of NO produced from the experiment with blank reactor (see figure 4.10) is lower than the amount observed with reactor packed with catalyst. Therefore, there is another catalytic oxidation reaction of NH_3 occurs co-currently with the homogeneous reaction. The possible mechanism for this catalytic reaction is REDOX model. In this model NH_3 reacts with lattice oxygen (O^{2-}) of the catalyst to form N_2O and H_2O. Then gaseous O_2 reoxidized the catalyst surface back to its original state.

4.4 Conclusions

From the experimental results illustrated in this chapter, the following conclusions can be drawn.

1. N_2O is produced from the reaction between NH_3 and NO
2. In the low reaction temperature region, the reaction proceed via Eley-Rideal mechanism.
3. In the high reaction temperature region, the reaction likely proceeds via REDOX mechanism.
4. Since at high temperature, NH_3 barely exists on the catalyst surface. The oxidation of NH_3 should be proceeding via REDOX mechanism and homogeneous reaction.

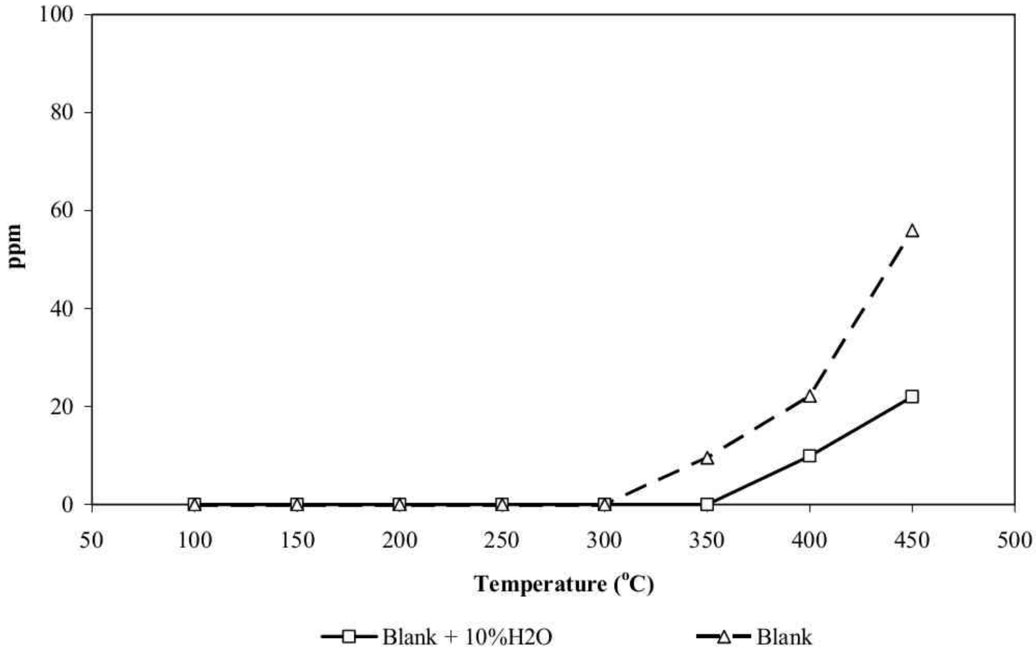

Figure 4.10 The NH_3 oxidation in blank reactor for SCR of NO with NH_3. (Keawbuddee, 2010)

CHAPTER V

CONCLUSIONS

This chapter shows the conclusions obtained from the experimental results. From the experimental results reported and the discussion in the previous chapter the following conclusions can be drawn:

5.1 Conclusions

1. The selective catalytic reduction process followed by Eley-Rideal Mechanism. Because of this mechanism, signifies catalytic of selective catalytic reduction at low reaction temperature, but higher reaction temperature the amount of NH_3 adsorption on the catalyst surface determined how much NO conversion can be achieve.

2. N_2O occurred from NO react with adsorb NH_3 on the catalyst surface following the Eley-Rideal mechanism.

3. Decreasing amount of W content tends to increases the amount of N_2O, but decreasing amount of Mo content was less affected.

4. NH_3 oxidation occurred while via homogeneous reaction, NH_3 in gas phase react with O_2, and be REDOX mechanism.

5. The oxidation of SO_2 to SO_3 does not occur.

5.2 Recommendations for future work

1. Study the removal N_2O by selective catalytic reduction with NH_3.
2. Improve a catalyst which minimizes production N_2O occur during the selective catalytic reduction of NO with NH_3

REFERENCES

Amiridis, M.D., Wachs, I.E., Deo, G., Jehng, J.M. and Kimy, D.S. reactivity of V_2O_5 Catalysts for the Selective Catalytic Reduction of NO by NH_3: Influence of Vanadia Loading, H_2O, and SO_2. Journal of catalysis 161 (1996): 247-253.

Bartholomew, C.H., Farrauto, R.J. Catalytic Reduction of NO_x. Fundamentals of Industrial Catalytic Processes (2010): 756, 777.

Beretta A., Orsenigo G., Ferlazzo N., Tronconi E. and Forzatti P. Analysis of the performance of plate-type monolithic catalysts for selective catalytic reduction deNOx applications. Ind. Eng. Chem. Res. 37 (1998): 2623-2633.

Bond, G.C. Heterogeneous Catalysis, Principles and applications, pp 38-47. Oxford : University Press, 1987.

Bosch, H. and Janssen, F. Formation and control of nitrogen oxides. Catal Today 23 (1988): 69-79.

Boyano, A., and others. A comparative study of V_2O_5/AC and V_2O_5/ Al_2O_3 Catalysts for the selective catalytic reduction of NO byNH_3. Chemical Engineering Journal 149 (2009):173-182

Casagrande, L., Lietti, L., Nova, I., Forzatti, P., Baiker, A. SCR of NO by NH_3 over TiO_2-supported V_2O_5-MoO_3 catalysts reactivity and redox behavior. Applied Catalysis B: Environmental 22 (1999): 63-77.

Chen, J. and Yang, R. Catal.A:General 80 (1992): 135.

Chen, L., Li, J. and GE, M. The poisoning effect of alkali metals doping over nano V_2O_3-WO_3/TiO_2 catalysts on SCR of NO_x by NH_3. Chemical Engineering Journal 170 (2011):531-537

Delahay, G., Coq, B., Kieger, S., Neveu, B. The origin of N_2O formation in the selective catalytic reduction of NO_x by NH_3 in O_2 rich atmosphere on Cu-faojasite catalysts. Catalysis Today (1999): 431-438

Gabrielsson, P. and Pedersen, H.G. Flue Gas from Stationary Sources. Handbook of Heterogeneous Catalysis 2 (2008): 2349

Guo, X., Bartholomew, C., Hecker, W. and Baxter, L. Effects of sulfate species on V_2O_5/TiO_2 SCR catalysts in coal and biomass-fired systems. Applied Catalysis B: Environmental 92 (2009) 30-40.

Gao, X., Jiang, Y., Zhong, Y., Luo, Z., Cen, K. The activity and characterization of CeO_2-TiO_2 Catalysts prepared by the sol-gel method for SCR. Journal of Hazardous Materials, 174 (2010):734-739

Haitao, X., and others. A novel catalyst of silicon cerium complex oxides for SCR of NO by NH_3. Journal of rare earth 28 (2010):721

Huang Z., Zhu Z. and Liu Z. Combined effect of H_2O and SO_2 on V_2O_5/AC catalysts for NO reduction with ammonia at lower temperatures. Applied Catalysis B: Environmental 39 (2002): 361–368.

Jung S. M. and Grange P., DRIFTS investigation of V=O behavior and its relations with the reactivity of ammonia oxidation and selective catalytic reduction of NO over V_2O_5 catalyst. Applied Catalysis B: Environmental 36 (2002): 325–332.

Kamata, H., Ohara, H., Takahashi, K., Yukimura A. and Seo, Y. SO_2 oxidation over the V_2O_5/TiO_2 SCR catalyst. Catalysis Letters 73 (2001): 79-83.

Kaewbuddee C. Selective catalytic reduction (SCR) of nitrogen oxide by ammonia over V_2O_5-WO_3/TiO_2 catalysts. Mater's Thesis, Department of Chemical Engineering, Faculty of Engineering, Chulalongkorn university 2009.

Lee, X., Kim, X. and Hong, S. Systematic mechanism study of the high temperature SCR of NO_x by NH_3 over a W/TiO_2 catalyst. Chemical Engineering Science 79 (2012):177-185

Mars, P. and van Krevelen, D.W., Chem. Eng. Sci. (Spec. Suppl.), 3, (1954) 51-59.

Mongkhonsi, T. and Kaewbuddee, C. Selective Catalytic Reduction of NO in Gas Turbine Exhaust Gas with NH_3. Pathumwan Academic Journal 5 (2012) 1-9

Nova I., Liettia L.,Casagrandea L., Dall'Acquab L., Giamellob E. and Forzatti P. Characterization and reactivity of TiO_2-supported MoO_3 De-NO_x SCR catalysts. Applied Catalysis B: Environmental 17 (1998): 245-258.

Orsenigo C., Lietti L., Tronconi E., Forzatti P. and Bregani F. Dynamic investigation of the role of the surface sulfates in NO_X reduction and SO_2 oxidation over V_2O_5-WO_3/TiO_2 catalysts. Ind. Eng. Chem. Res. 37 (1998): 2350-2359.

Piyanantaruk B. Selective catalytic reduction of nitrogen oxide by ammonia over V_2O_5-WO_3-MoO_3/TiO_2 catalysts. Master's Thesis, Department of Chemical Engineering, Faculty of Engineering, Chulalongkorn university 2011.

Qi G. and Yang R.T. Low-temperature selective catalytic reduction of NO with NH_3 over iron and manganese oxides supported on titania. Applied Catalysis B: Environmental 44 (2003): 217–225.

Taweesuk B. Selective catalytic reduction (SCR) of nitrogen oxide by ammonia over V_2O_5-MoO_3/TiO_2 catalysts. Master’s Thesis, Department of Chemical Engineering, Faculty of Engineering, Chulalongkorn university 2011.

Shen, B., Liu, T., Zhao, N., Yang, X., Deng, L. Iron-doped Mn-Ce/TiO_2 catalyst for low temperature SCR of NO with NH_3. Journal of Environmental Sciences (2010):1447-1454

Warinsiririux K. Selective catalytic reduction of nitrogen oxide by ammonia over V_2O_5/TiO_2 containing WO_3 and MoO_3 catalysts. Master’s Thesis, Department of Chemical Engineering, Faculty of Engineering, Chulalongkorn university 2011.

Xiaodong, W., Zhichun, S., Guo, L., Duan, W., Ziran, M. Effects of cerium and vanadium on the activity and selectivity of MnO_x-TiO_2 catalyst for low-temperature NH_3-SCR. Journal of Rare Earths. 29 (2011):64-68

Xu, X., and others. Tungsten modified MnO_x-CeO_2/ZrO_2 monolith catalysts for SCR of NO_x by NH_3. Chemical Engineering Science 76 (2012):120-128

APPENDICES

APPENDIX A

CALIBRATING DATA FOR MASS FLOW METER

A1 Calibration data of mass flow meter are shown as follows:

Component of feed gas mixture: ammonia, nitrogen oxide, nitrogen, oxygen and sulfur dioxide

A1.1 Calibration for ammonia mass flow controller

Use the bubble flow by passing the gas through the glass tube in order to measure the time. Recording the time from scale 0 ml to 5 ml of the tube.

Table A1 Calibration data of ammonia mass flow controller.

Mass flow meter scale (ml/min)	Time (sec)			Time average (sec)	Actual flow (ml/min)
	#1	#2	#3		
1	54.62	54.91	55.91	55.15	2.18
2	25.03	24.91	24.88	24.94	4.81
3	16.09	15.69	15.84	15.87	7.56
4	11.97	11.84	11.87	11.89	10.09
5	9.38	9.47	9.38	9.41	12.75

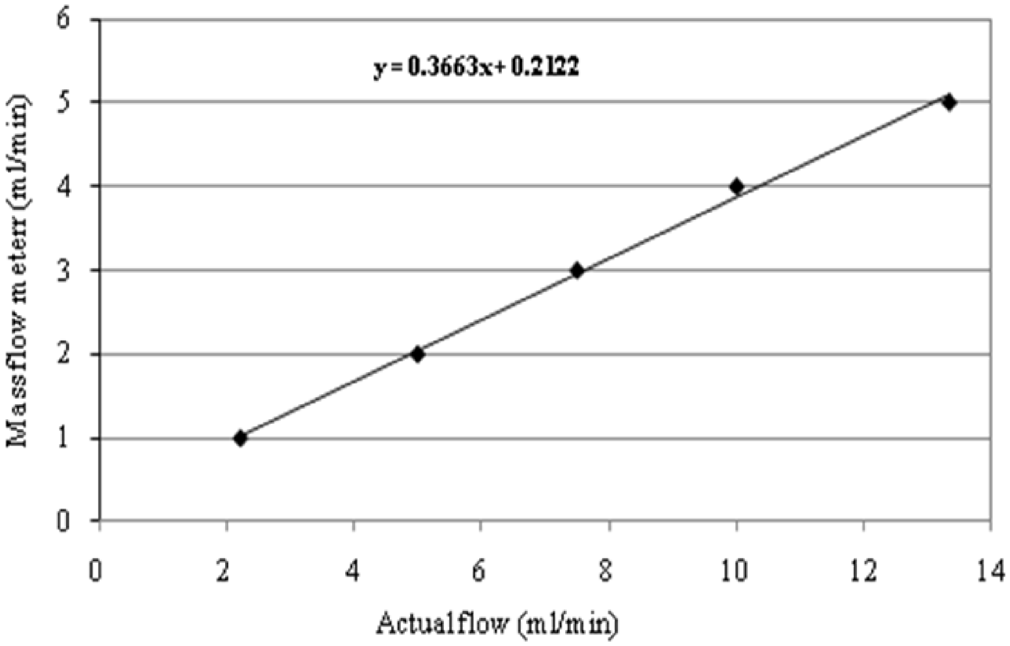

Figure A1 Calibration curve of ammonia mass flow controller

A1.2 Calibration for nitrogen oxide mass flow controller

Use the bubble flow by passing the gas through the glass tube in order to measure the time. Recording the time from scale 0 ml to 5 ml of the tube.

Table A2 Calibration data of nitrogen oxide mass flow controller.

Mass flow meter (ml/min)	**Time (sec)**			**Time average (sec)**	**Actual flow (ml/min)**
	#1	**#2**	**#3**		
1	75.38	80.25	75.97	77.20	1.43
2	34.22	35.00	37.75	35.66	3.09
3	22.82	23.78	23.37	23.32	4.73
4	17.50	17.37	18.04	17.64	6.37
5	13.78	13.47	14.16	13.80	7.81

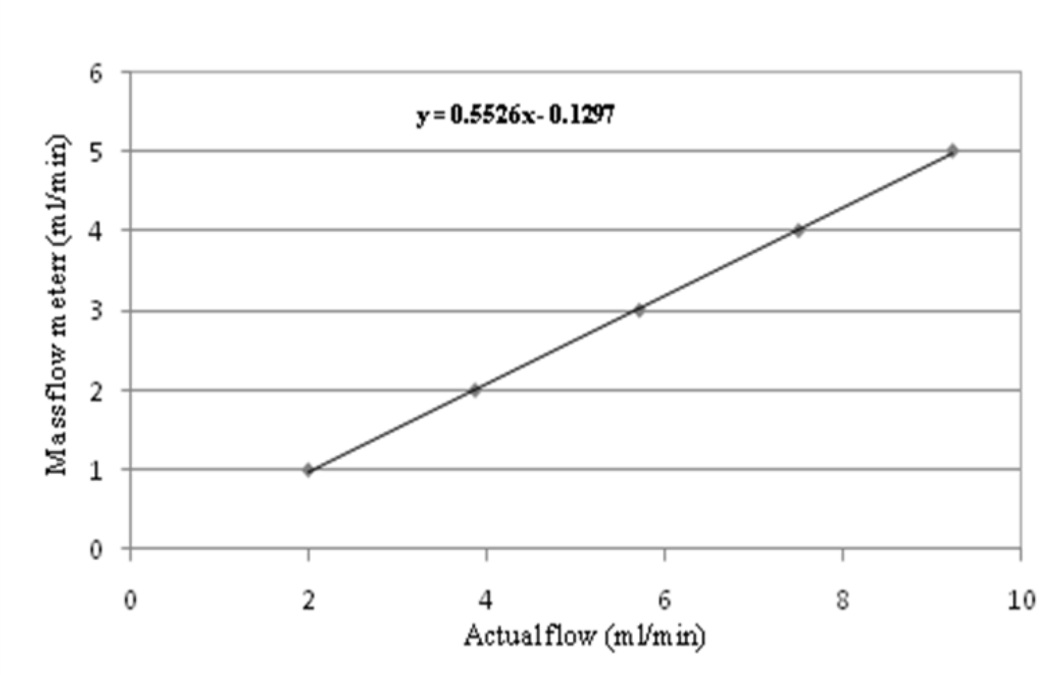

Figure A2 Calibration curve of nitrogen oxide mass flow controller.

A1.3 Calibration for oxygen mass flow controller

Use the bubble flow by passing the gas through the glass tube in order to measure the time. Record the time from scale 0 ml to 5 ml of the tube.

Table A3 Calibration data of oxygen mass flow controller.

Mass flow meter (ml/min)	Time (sec)			Time average (sec)	Actual flow (ml/min)
	#1	#2	#3		
10	55.56	55.50	55.44	55.50	10.81
20	28.00	27.97	28.00	27.99	21.44
30	18.85	18.75	18.44	18.68	32.12
40	14.07	14.10	14.03	14.07	42.65
50	11.13	11.18	11.25	11.19	53.64

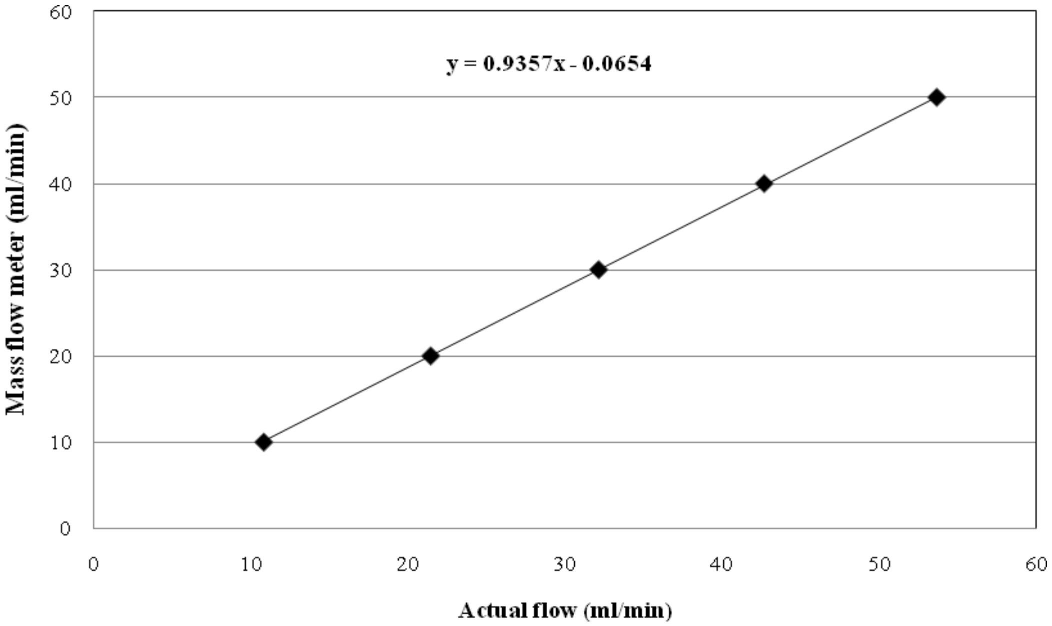

Figure A3 Calibration curve of oxygen mass flow controller.

A1.4 Calibration for nitrogen mass flow controller

Use the bubble flow by passing the gas through the glass tube in order to measure the time. Recording the time from scale 0 ml to 5 ml of the tube.

Table A4 Calibration data of nitrogen mass flow controller.

Mass flow meter (ml/min)	**Time (sec)**			**Time average (sec)**	**Actual flow (ml/min)**
	#1	**#2**	**#3**		
150	8	8	8	8	147
160	8	8	8	8	157
170	7	7	7	7	165
180	7	7	7	7	176
190	7	6	6	6	187

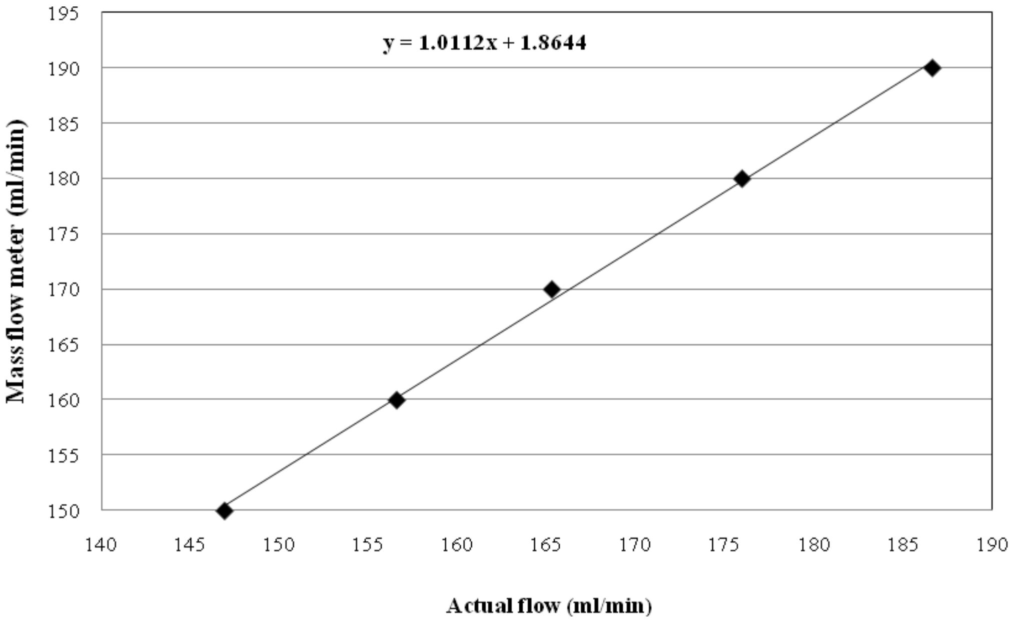

Figure A4 Calibration curve of nitrogen mass flow controller.

A1.5 Calibration for sulfur dioxide mass flow controller

Use the bubble flow by passing the gas through the glass tube in order to measure the time. Recording the time from scale 0 ml to 5 ml of the tube.

Table A5 Calibration data of sulfur dioxide mass flow controller.

Mass flow meter (ml/min)	Time (sec)			Time average (sec)	Actual flow (ml/min)
	#1	#2	#3		
1	84.9	82.5	83.59	83.66	1.43
2	38.72	38.65	39.06	38.81	3.09
3	25.34	25.50	25.31	25.38	4.73
4	18.75	18.84	18.94	18.84	6.37
5	15.32	15.43	15.37	15.37	7.81

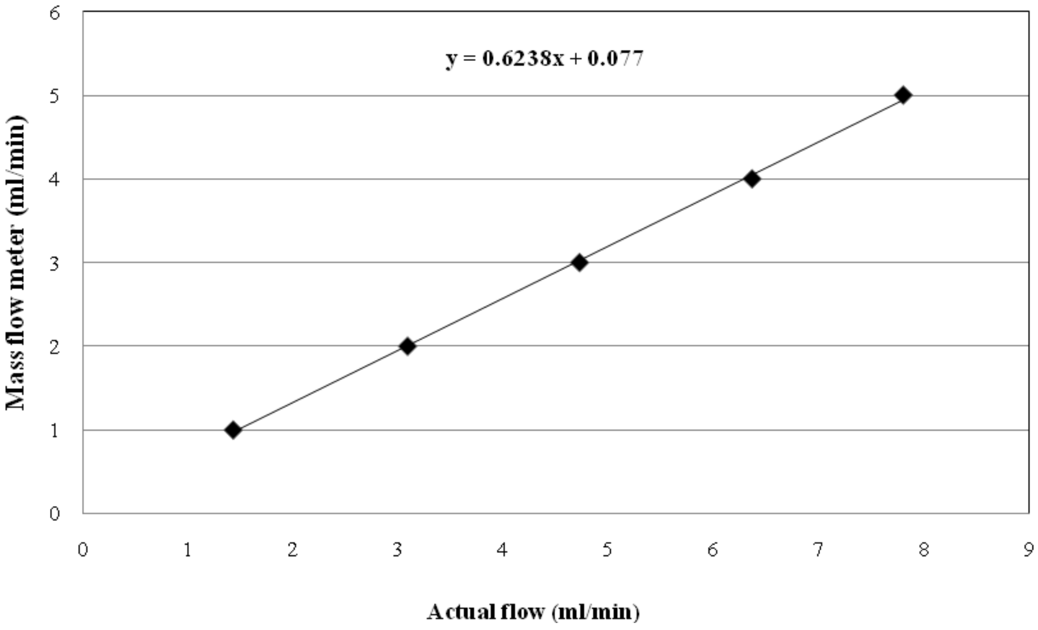

Figure A5 Calibration curve of sulfur dioxide mass flow controller

APPENDIX B

CALCULATION FOR CATALYST PREPARATION

Preparation of V_2O_5-WO_3-MoO_3/TiO_2 catalyst is shown as follows:

Reagent:

- Titania powder prepared by a sol-gel method
- Ammonium metavanadate 99.999%
  NH_4VO_3 (Aldrich)
- Ammonium metatungsteae hydrate 99.99%
  $(NH_4)_6H_2W_{12}O_{40}\bullet xH_{2O}$ (Aldrich)
- Ammonium heptamolybdate
  $(NH_4)_6Mo_7O_{24}\bullet 4H_2O$ (Aldrich)
- Oxalic acid hydrate (Fluka)

Calculation for the preparation of V_2O_5-WO_3-MoO_3/TiO_2

Example calculation for the preparation of 3 wt. %V_2O_5-7 wt. %WO_3-10 wt. %MoO_3

Based on 2 g of catalyst used, the composition of the catalyst will be as follows:

V_2O_5 = 0.03×2 = 0.06 g
WO_3 = 0.07×2 = 0.14 g
MoO_3 = 0.06×2 = 0.12 g
TiO_2 = 2 - 0.06 - 0.14 - 0.12 = 1.60 g

Vanadium oxide 0.06 g was prepared from NH_4VO_3 and molecular weight of V_2O_5 is 180.39 g/mole.

$$NH_4VO_3 \text{ required} = \frac{(NH_4)_2VO_3 \times \text{tungsten oxide required x 2}}{\text{MW of } V_2O_5}$$

$$= \frac{116.98 \times 0.06 \times 2}{180.39} = 0.0778 \text{ g}$$

Tungsten oxide 0.14 g was prepared from $(NH_4)_6H_2W_{12}O_{40}{\bullet}xH_2O$ and molecular weight of WO_3 is 231.84 g/mole.

$$(NH_4)_6H_2W_{12}O_{40}{\bullet}xH_2O = \frac{(NH_4)_6H_2W_{12}O_{40}.xH_2O \times \text{tungsten oxide required}}{12 \times \text{MW of } WO_3}$$

$$= \frac{2956.3 \times 0.14}{231.84 \times 12} = 0.1488 \text{ g}$$

Molybdenum oxide 0.12 g was prepared from $(NH_4)MoO_4$ and molecular weight of MoO_3 is 143.94 g/mole

$$(NH_4)_2MoO_4 = \frac{(NH_4)_2MoO_4 \times \text{molybdenum oxide required}}{\text{MW of } MoO_3}$$

$$= \frac{196.02 \times 0.2}{143.94} = 0.2724 \text{ g}$$

Oxalic acid require

Mole of vanadium oxide = 0.06/180.39 = 0.000333 mole

Molecular weight of oxalic acid equal to 126.07 g/mole.

Oxalic acid required = 0.000333×126.07 = 0.0416

APPENDIX C

SHIMADZU GC-2014

Table C1 The operating condition of Shimadzu GC-2014.

Shimadzu GC-2014	**Analyzed gas**		
	NO	**N_2O**	**SO_2**
Detector	ECD	ECD	FPD
Temp Detector (°C)	200	200	185
Column	Hyasep-DB	Hyasep-DB	Rt-XL sulfur
Max temperature column (°C)	190	190	240
Temperature column (°C)	40	150	180
Inner Diameter column (mm)	0.1	0.1	1
Length column (m)	2	2	2
Temperature injector (°C)	-	-	100
Carrier gas	N_2	N_2	He
Carrier gas flow	240 kPa	240 kPa	15ml/min
Add flow (kPa)	-	-	Air:35 H_2:105
Sampling rate (msec)	80	80	40

ECD: Electron Capture Detector **FPD: Frame Photometric Detector**

APPENDIX D

LIST OF PUBLICATION

กมลทิพย์ แซ่บ้าง, เกียรติลดา วารินศิริรักษ์ และ ธราธร มงคลศรี. ผลของลำดับการเติมโลหะต่อความว่องไวของตัวเร่งปฏิกิริยาโลหะออกไซด์ผสม V-W-Mo บนตัวรองรับ TiO_2 สำหรับการรีดิวซ์แบบเลือกเกิดของแก๊ส NO ด้วยแก๊ส NH_3 การประชุมวิชาการวิศวกรรมเคมีและเคมีประยุกต์แห่งประเทศไทย, ครั้งที่ 22, 25 – 26 ตุลาคม 2555, ณ โรงแรมเดอะกรีนเนอรี่รีสอร์ท จ. นครราชสีมา, Ref. NO. TCR-08

VITA

Miss Kamoltip Saebang was born on November 03, 1988 in Nakhonsi thammarat, Thailand. She finished high school from Triam Udom Suksa School of the South, Nakhonsithammarat, and graduated the bachelor's degree of Chemical Engineering, Rajamankala University of Technology Thunyaburi, in academic year 2010. She continued her master's study at Department of Chemical Engineering, Faculty of Engineering, Chulalongkorn University in 2011.